UCID- 20285-2

Interim Technical Report No. 2 for Materials Synthesis Program

1 February 1985 to 1 June 1985

J. B. Holt

July 1985

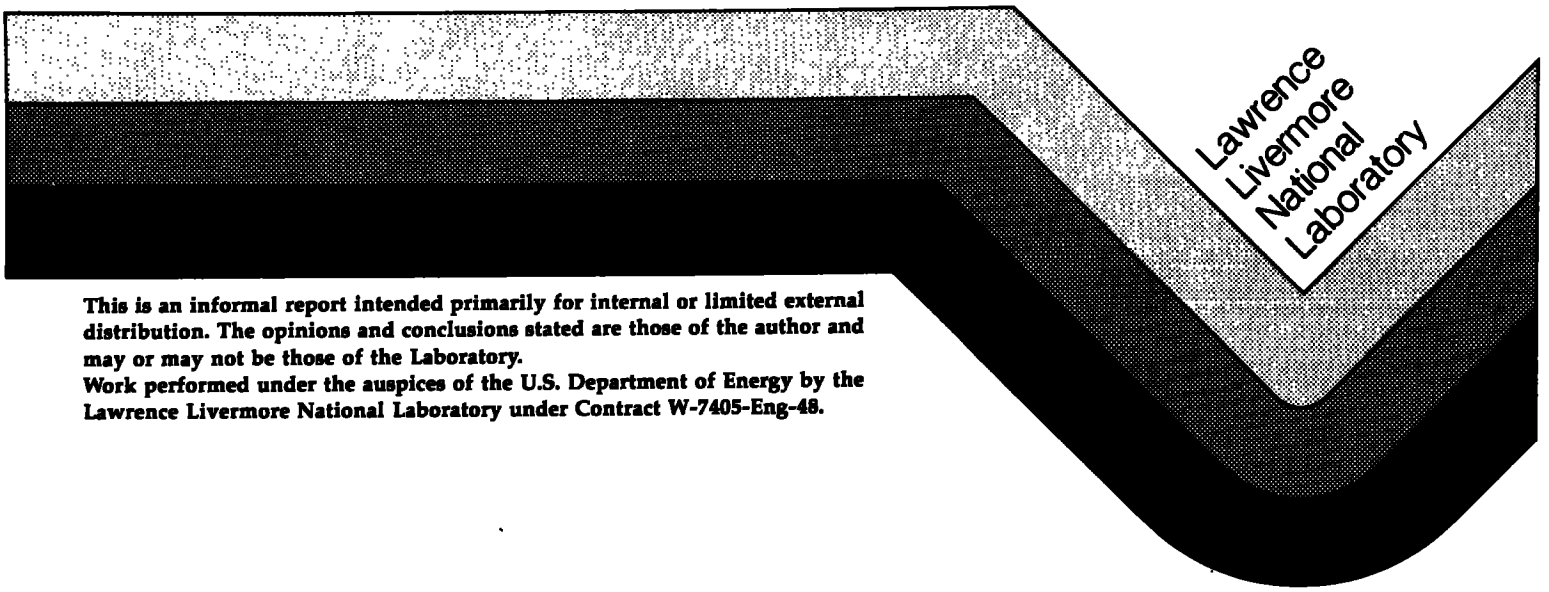

Work performed under the auspices of the U.S. Department of Energy by the Lawrence Livermore National Laboratory under Contract W-7405-Eng-48.

Printed in the United States of America
Available from
National Technical Information Service
U.S. Department of Commerce
5285 Port Royal Road
Springfield, VA 22161
Price: Printed Copy $; Microfiche $4.50

Page Range	Domestic Price	Page Range	Domestic Price
001-025	$ 7.00	326-350	$ 26.50
026-050	8.50	351-375	28.00
051-075	10.00	376-400	29.50
076-100	11.50	401-426	31.00
101-125	13.00	427-450	32.50
126-150	14.50	451-475	34.00
151-175	16.00	476-500	35.50
176-200	17.50	501-525	37.00
201-225	19.00	526-550	38.50
226-250	20.50	551-575	40.00
251-275	22.00	576-600	41.50
276-300	23.50	601-up[1]	
301-325	25.00		

[1]Add 1.50 for each additional 25 page increment, or portion thereof from 601 pages up.

Interim Technical Report No. 2 for

Materials Synthesis Program*

For the Period 1 February 1985 to 1 June 1985

by

J. B. Holt

Lawrence Livermore National Laboratory
Livermore, California 94550

Sponsored by

Defense Advanced Research Projects Agency (DoD)
Materials Sciences Division/Defense Sciences Office
Synthesis of Advanced Materials Program
ARPA Order No. 5051

Issued by

U.S. Army Materials and Mechanics Research Center
Under MIPR # 84-5051-01

*The views and conclusions contained in this document are those of the authors and should not be interpreted as representing the official policies, either expressed or implied, of the Defense Advanced Research Projects Agency or the U.S. Government.

CONTENTS

UNCLASSIFIED
SECURITY CLASSIFICATION OF THIS PAGE

REPORT DOCUMENTATION PAGE

1a. REPORT SECURITY CLASSIFICATION UNCLASSIFIED	1b. RESTRICTIVE MARKINGS
2a. SECURITY CLASSIFICATION AUTHORITY	3. DISTRIBUTION / AVAILABILITY OF REPORT Approved for public release; distribution unlimited
2b. DECLASSIFICATION / DOWNGRADING SCHEDULE	
4. PERFORMING ORGANIZATION REPORT NUMBER(S) UCID 20285-2	5. MONITORING ORGANIZATION REPORT NUMBER(S)
6a. NAME OF PERFORMING ORGANIZATION Lawrence Livermore National Laboratory 6b. OFFICE SYMBOL (If applicable)	7a. NAME OF MONITORING ORGANIZATION U. S. Army Materials & Mechanics Research Center
6c. ADDRESS (City, State, and ZIP Code) P. O. Box 808 L-369 Livermore, CA 94550	7b. ADDRESS (City, State, and ZIP Code) Watertown, MA 02172
8a. NAME OF FUNDING / SPONSORING ORGANIZATION DARPA 8b. OFFICE SYMBOL (If applicable)	9. PROCUREMENT INSTRUMENT IDENTIFICATION NUMBER
8c. ADDRESS (City, State, and ZIP Code) 1400 Wilson Blvd. Arlington, VA 22209	10. SOURCE OF FUNDING NUMBERS PROGRAM ELEMENT NO. 61101E; PROJECT NO. ARPA AO 5051; TASK NO. 4D10; WORK UNIT ACCESSION NO. 002AW

11. TITLE (Include Security Classification)

Interim Technical Report No. 2 - Materials Synthesis Program (U)

12. PERSONAL AUTHOR(S)

J. B. Holt

13a. TYPE OF REPORT	13b. TIME COVERED	14. DATE OF REPORT (Year, Month, Day)	15. PAGE COUNT
Progress	FROM 2/85 TO 6/85	1985, July 15	57

16. SUPPLEMENTARY NOTATION

17. COSATI CODES			18. SUBJECT TERMS (Continue on reverse if necessary and identify by block number)
FIELD	GROUP	SUB-GROUP	

19. ABSTRACT (Continue on reverse if necessary and identify by block number)

20. DISTRIBUTION / AVAILABILITY OF ABSTRACT ☐ UNCLASSIFIED/UNLIMITED ☐ SAME AS RPT. ☐ DTIC USERS	21. ABSTRACT SECURITY CLASSIFICATION
22a. NAME OF RESPONSIBLE INDIVIDUAL	22b. TELEPHONE (Include Area Code) / 22c. OFFICE SYMBOL

DD FORM 1473, 84 MAR 83 APR edition may be used until exhausted. All other editions are obsolete.

SECURITY CLASSIFICATION OF THIS PAGE

EXECUTIVE SUMMARY/ABSTRACT

The objective of this research is to understand the mechanism of solid state combustion so that cost effective processes may be developed to produce fully dense parts of refractory borides, carbides and nitrides. This rather broad goal has been separated into smaller specific tasks.

The first task is a fundamental study of the kinetics of combustion of Ti-B and Ti-C systems to provide data on the experimental parameters which influence the structure of the products. Combustion wave velocities and temperatures have been measured in the Ti-B system. Preliminary data on the Ti-2B and Ti-1.5B compositions indicate activation energies of 539 kJ/mole and 410 kJ/mole respectively. For the Ti-2B reaction, our calculated value is 288 kJ/mole higher than the activation energy determined by Merzhanov (8). In future experiments as the temperature range is expanded and other variables are investigated then we may be able to resolve this large difference in activation energies. There is no other data available on the combustion of Ti-1.5B. The Ti-1.5 composition was selected for study because the product at temperature should consist of a solid TiB_2 phase in a molten TiB matrix. The molten phase should enhance the densification process by analogy to liquid phase sintering. However, no increase in the final density was observed, thus emphasizing the strong effect of outgassing on the density of the product.

To better understand the mechanism of combustion additional data on the temperature profile of the combustion wave front is required. Data acquisition equipment capable of measuring and analyzing signals from rapid response thermocouples are now a part of our facilities. Our initial profiles recorded on a oscilloscope were strongly influenced by the size of the thermocouple bead and thermoelectric effects.

In support of this fundamental study of the solid state combustion process the Ni-Al reaction was chosen as a model system for investigating densification during combustion. Under the direction of Professor Zuhair Munir at the University of California at Davis, Kathy Philpot, a graduate student, began a study of the pre-combustion processes in the Ni-Al system. Ni-Al mixtures in the range of 5-30 at.% Al were studied by varying the rate of heating from 1 to 5°C/min. In this case ignition occurs throughout the mixture at the same time so that the movement of a combustion wave was not a part of the combustion reaction. The major compound in the product was $AlNi_3$. At the lowest rate of heating ($\sim$1°/min) $AlNi_3$ was formed in the solid state by a series of reactions involving Al_3Ni and Al_3Ni_2. When the rate was raised to 5°C/min. the $AlNi_3$ was formed by liquid-solid reaction between molten Al and solid Ni. The types of product formed were related to rate of heating, chemical composition and size of the powders.

Robert Behrens, at LANL, in cooperation with Professor John Margrave of Rice University, will study ignition which is an important step in the overall combustion process. Powder mixtures of Ti-C, Ti-1.5B, Zr-B, Zr-C, Hf-C and Hf-B have been prepared for study at Houston Area Research Center (HARC). Mass spectrometry will be used to identify the gaseous species, both condensible and non-condensable, evolved during ignition.

The other two tasks are directed to the development of combustion processes to form refractory products. Since the combustion temperature of most reactions of interest are below the melting point temperature of the product then the form of the product will be either a powder or porous solid. By combining the combustion process with high pressure techniques new processes for synthesizing non-oxide materials are under investigation. Previous study has shown that TiC and TiB_2 can be densified to 95 and 97% of theoretical density respectively by application of 2,000 psi immediately after reaction in a graphite die. The use of isostatic pressure should provide for larger parts to be fabricated. Our efforts to synthesize TiB_2 parts by isostatic pressure have been hampered by the adsorbed gases on the reactant powders. Even at 15,000 psi tantalum cans burst by the build-up of pressure as the volume within the can is reduced. Study of this method will continue by degassing the powders prior to combustion. Another high pressure method is to initiate combustion and densify the product in the same step by shock waves generated by explosives. Experiments have shown that the reaction of $Ti + 2B = TiB_2$ can be initiated but the steel dies have blown apart. The die design has changed several times so that the product may be retained. Shock wave pressures over 150 kilobar are required to ignite the combustion reaction for producing TiB_2.

The third task is the development of the combustion process to form the refractory nitrides such as Si_3N_4, AlN etc. In prior experiments the procedures for synthesizing TiN, HfN, ZrN and ScN were established for use as a commercial process. The method which utilizes NaN_3 as a solid source of nitrogen, was not directly applicable to the other technologically important nitrides. Now the processes have been defined by which Si_3N_4, AlN, BN, TaN and β' Sialon have been synthesized. The optimum processes for full conversion are under study along with a characterization of the products.

Another application of solid state combustion to produce sinterable powders is being investigated by Raymond Cutler of Cermatec. His work is centered on thermite-type reactions to produce fine submicron powder capable of being sintered. SiC may be prepared by the following reaction:

$$SiO_2 + 2Mg + C = SiC = 2MgO \qquad (1)$$

The MgO is leached out by a hydrochloric acid solution to leave a fine SiC powder. It appears that the particle size of the carbon powder controls the ultimate particle size of the SiC product. The initial size of SiO_2 is important since large SiO_2 particles do not form SiC. On the basis of these experimental observations it seems possible that combustion processes can be developed to produce submicron powders of such valuable materials as SiC and TiC.

SECTION I

J. Birch Holt
Lawrence Livermore National Laboratory

COMBUSTION SYNTHESIS

INTRODUCTION

When a solid chemically reacts with another solid or gas, the reaction is usually accompanied by the evolution of heat. The amount of heat evolved in these exothermic reactions may raise the product to high temperatures which will cause the self propogation of a combustion wave. Many refractory compounds possess high heats of reaction such as 1300 cal/g, and 962 cal/g for TiN and TiB_2, respectively.

In the synthesis of nonoxide refractory materials by conventional production methods the chemical reaction between powders is initiated by heat from an external source such as a furnace. The rate of heat-up in a furnace is purposely kept low to prevent any high temperature exclusions caused by the high heat of reaction. Refractory compounds, such as carbides and borides, prepared in this manner are relatively expensive because of the high cost of energy.

Another way to initiate these chemical reactions is by heating a small surface area to the ignition point. The expenditure of energy is very small in this case and may be supplied by a pulsed laser, radiation lamp, electric match, heated surface, etc. If the reaction is sufficiently exothermic, then a combustion wave will spontaneously propagate through the powder reactants leaving behind the product phase. Unique features of the self-propagating reaction are high temperatures (2000°C-4000°C), rapidly moving combustion waves, and high rates of heating and cooling at the combustion front.

Russian Scientists, guided by A. G. Merzhanov [1,2,3], developed the self-propagating high temperature synthesis (SHS) process to produce commercial materials. Their initial emphasis was on the synthesis of refractory powders. $MoSi_2$, TiC, SiC, Si_3N_4, TiB_2 among others are produced in large quantities. They recognized that the optimum process was not to produce powders but fully dense parts. Recent papers [4,5] indicate that the direction of their research and development effort is toward an integrated process that combines synthesis and densification.

Our research on the solid combustion process started about three years ago. The first phase of our effort was to verify some of the experimental parameters in the combustion of simple systems such as $Ti + C \rightarrow TiC$ and $Ti + 2B \rightarrow TiB_2$. Our findings verified the basic concepts of solid state combustion and demonstrated the great potential of these types of reactions to produce refractory compounds. The extensive research of the Russian scientists, both theoretical and experimental, laid a foundation for the use of the SHS process to produce refractory materials. With this information we concentrated our research on those areas which offer opportunities for new applications.

Consequently, the research on Solid State Combustion processes at LLNL has been directed into three tasks. The first task is a fundamental study of the kinetics of the combustion process to gain a greater understanding of the

mechanism of combustion and the experimental parameters which might affect the structure of the product. The other two tasks are application oriented. The second task is the Simultaneous Synthesis and Densification of Combustion Products. Our early research strongly indicated that the most attractive commercial process would combine synthesis and densification into one step in agreement with the emphasis of Russian research. The third task is a research and development effort to synthesize some of the technologically important nitrides such as Si_3N_4, AlN, and BN. Our previous research demonstrated that the transition metal nitrides could be easily prepared by using NaN_3 as a solid source of nitrogen. However, this technique was not directly applicable to Si_3N_4, AlN and BN. Consequently, we have developed other experimental procedures for synthesis of these nitrides by combustion.

In support of these research objectives other investigators have been selected to study different aspects of the combustion process. Dr. Raymond Cutler of Ceramatec, Inc. is studying thermite-type reactions to form a submicron sinterable SiC powder. This is an intriguing variation to the combustion reaction between metals and nonmetals. Another chemical system that he is studying is $TiC-Al_2O_3$ and the prospects for its commercial applications seem very promising.

Kathy Philpot, a graduate student at the University of California at Davis, has been investigating the combustion of Ni-Al powder mixtures as a model for precombustion processes. Not only has her work produced data which might be applied to more refractory materials but the results may provide the experimental parameters necessary to prepare Ni-Al alloys by the combustion process.

There are many aspects of the ignition step in combustion reactions which remain unclear. For example, what effect do the impurity gases have on ignition temperature and to what extent is ignition controlled by the melting point of the lower melting reactant. Bob Behrens at LANL and John Margrave of Rice University are investigating the ignition of chemical systems such as TiC and TiB_2 that are important compounds in our material synthesis program.

TASK 1. KINETICS OF SOLID STATE COMBUSTION

INTRODUCTION

The general expression describing the constant velocity of a self-propagating combustion wave in a mixture of solid reactants is given by

$$\lambda \frac{d^2T}{dx^2} - \rho c u \frac{dT}{dx} + Q p \phi(T,\eta) = 0, \qquad (1)$$

where λ = thermal conductivity

T = temperature

c = heat capacity

ρ = density

u = wave velocity

Q = heat of reaction

η = fraction reacted

ϕ = kinetic function.

Boundary conditions are: $X = -\infty$ $T = T_o$ $\eta = 0$

$X = +\infty$ $T = T_c$ $\eta = 1$.

The third term on the left of equation (1) is the heat-generation term and contains the kinetic function of the combustion reaction. For a homogeneous reaction this function may be expressed by:

$$\phi(T,\eta) = \frac{ud\eta}{dx} = \frac{d\eta}{dt} = K_o\, e^{-E/RT}\, (1-\eta)^n, \qquad (2)$$

where K_o = pre-exponential factor

E = activation energy

n = order of reaction.

Using equation (2) as the kinetic function and assuming a narrow reaction zone and a 1st order reaction, the solution to equation (1) is equation (3).

$$u^2 = \sigma_n\, a\, \frac{c}{Q}\, \frac{RT^2}{E}\, K_o\, e^{-E/RT}, \qquad (3)$$

where K_o = constant depending on order of reaction

a = thermal diffusivity.

By measuring the combustion wave velocity as a function of combustion temperature then the activation energy may be computed from a plot of ln(u) versus 1/T. The combustion temperature is changed by heating the reactants with a furnace to raise T_o or the temperature is reduced by the addition of diluents.

Usually, most solid state reactions of the combustion type are not homogeneous reactions. Only when a liquid is formed or the reactant particles are very small and intimately mixed could solid state combustion be described as a homogeneous reaction. Nevertheless, even if the reaction was of the heterogeneous type the difference between the solutions as expressed in equation (3) would occur in the intercept term. A possible exception to this conclusion is an exponential heterogeneous reaction [6]. For this case the ln(u) versus 1/T plot would not be a linear function. The correct activation energy should be obtained from an Arrhenius plot regardless of whether the combustion process is a heterogeneous or homogeneous reaction.

Calculation of the activation energy however does not imply proof of the mechanism of combustion. Further experimental data is required before the particular mechanism of combustion i.e., diffusional, linear, cubic, etc., can be formulated with any confidence. This additional data is obtained from the

temperature profile of the combustion front. We are developing facilities and the experimental procedure to accurately measure high temperature profiles. Shown in Fig. 1 is a temperature profile of a combustion wave in a Ti-1.5B compact measured with a tungsten-rhenium thermocouple. Since the shape of the curve is strongly influenced by the size of the bead (response time) and thermoelectric effects then further refinement of the procedure is necessary before the recorded curve is an accurate display of the actual profile.

EXPERIMENTAL PROCEDURE

The Ti-B system system was selected for our initial studies based on the ease of ignition, technological importance of TiB_2, and the possibility to investigate the kinetics of two compounds: TiB and TiB_2. Our first measurements were made on mixtures of Ti-1.5B and Ti-2B. The Ti-1.5 mixture should react to form 0.5 mole TiB and 0.5 mole TiB_2. The melting point temperatures of TiB and TiB_2 are 2230°C and 2920°C, respectively. The actual combustion temperatures for the Ti-1.5B composition (Table 2) were between the melting point of the two compounds therefore, the product phase of the Ti-1.5B samples on combustion should be solid TiB_2 in a molten TiB matrix.

In preparation of the combustion samples titanium and boron powders were mechanically mixed for 15 minutes in a Spex mill. The characteristics of the powders are shown in Table 1. When the amorphous boron was used the components would expand up to 50% or fly apart on combustion. For this reason all of our experiments were conducted with the crystalline boron from Aldrich.

Ten to fifteen gram cylindrical compacts were cold-pressed, without additives, to approximately 60% of theoretical density. These compacts were burned in our combustion chamber under 1 atmosphere of argon. The ignition was accomplished by a heated tungsten coil. The velocity of the combustion wave was measured by high speed photography and the combustion temperature by a optical fiber (Ircon) focussed on a black body hole that had been placed in the sample near the midpoint of its length. In this first phase of our study no attempt was made to vary the initial compact density or reactant particle size.

RESULTS

The measured values of the velocities as a function of combustion temperatures are listed in Table 2. Data are presented for the combustion of both Ti-1.5 and Ti-2B samples. The temperature range was restricted because the addition of diluents in quantities greater than those listed caused the combustion wave to extinguish before reaching the bottom of the compact. A small furnace constructed of a quartz tube and tungsten elements was used to raise the T_o above room temperature. The result from heated samples have not been satisfactory since the additional temperature causes the sample to expand so that the optical fiber is no longer focussed on the black body hole. We are continuing on with these types of experiments to widen the range of combustion temperatures.

Another concern is the difference in mode of combustion as the temperature is decreased. As predicted by Merzhanov [6] and Margolis and Matkowsky [7] the mode of combustion will change from steady state to oscillatory to spin as the temperature of combustion decreased. We observed that at the lower tempera-

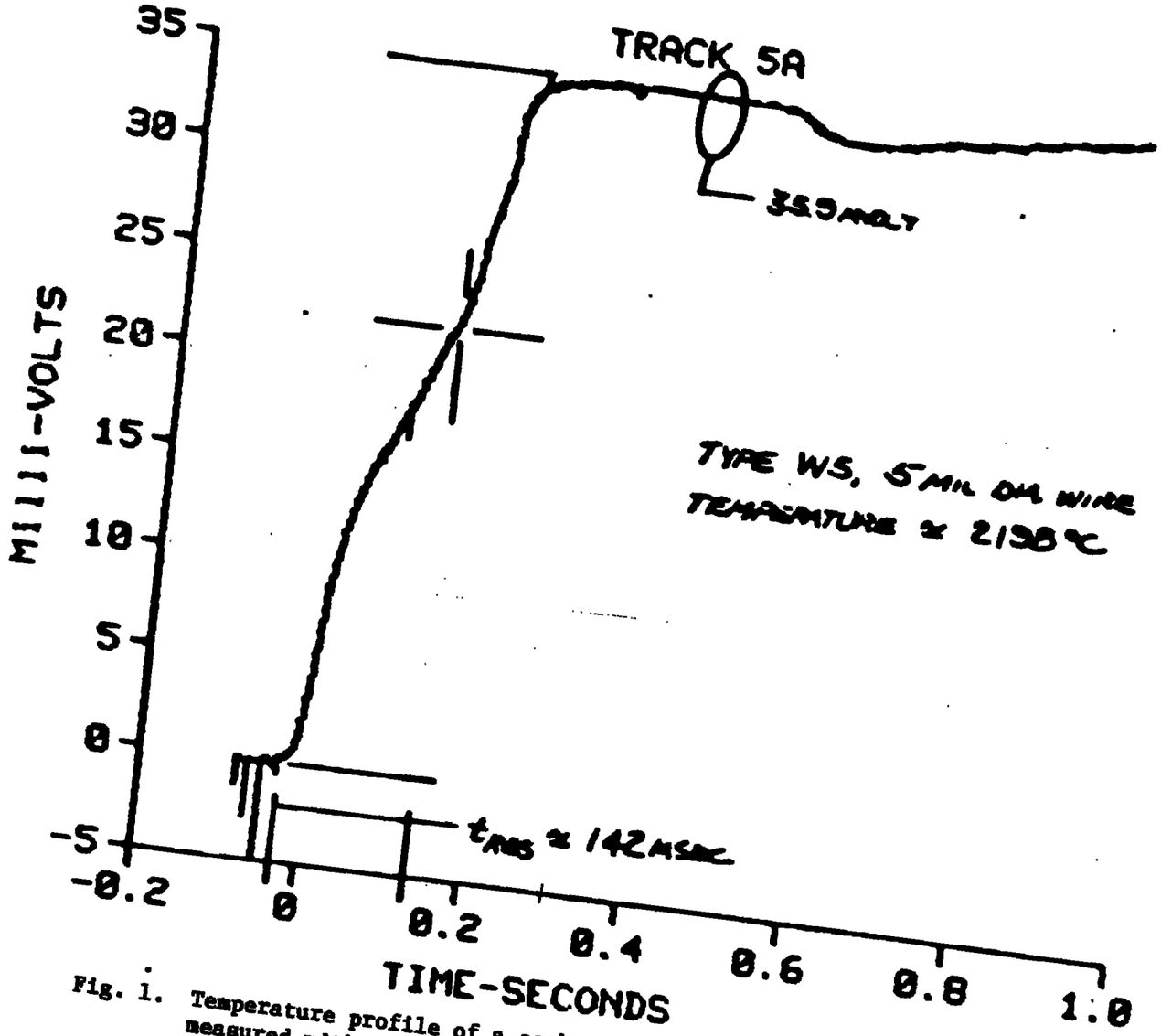

Fig. 1. Temperature profile of a combustion wave in a Ti-1.5B compact as measured with a W-WRe thermocouple. The maximum temperature was 2200°C and the width of the combustion zone approximately 3 mm.

TABLE 1. POWDER CHARACTERIZATION

Material	Surface Area (m^2/g)	Particle Size μ	Density (g/cm^3)
Ti (Alpha)	0.902	9.5	4.42
B (Aldrich, cry.)	11.15	1.6	2.18
B (Gallard, amorph.)	27.02	0.32	2.13

TABLE 2. KINETIC DATA FOR COMBUSTION OF Ti-1.5B AND Ti-2B

Material	Wt% Diluent (TiB_2)	Combustion Temperature °C	Wave Velocity (cm/s)
Ti-1.5B	0	2726	1.90
Ti-1.5B	5	2633	1.43
Ti-1.5B	10	2605	1.28
Ti-2B	10	2710	2.07
Ti-2B	12.5	2645	1.50
Ti-2B	20	2560	1.09

tures with both compositions that the movement of the front was unstable. Whether equation (3) can still be applied to these unstable burns is open to question since the assumption of steady state combustion was applied in its derivation.

When the data in Table 2 is plotted in Fig. 2, two activation energies are obtained: 539 kJ/mole for Ti-2B and 410 kJ/mole for Ti-1.5B. Also on the plot in Fig. 2 is a line representing the data for the combustion of Ti-2B as determined by Merzhanov [8]. His value of 318 kJ/mole is much lower than the 539 kJ/mole obtained in our experiments.

Unfortunately, there is very little kinetic data from other solid state reactions involving TiB_2. Pastor [9] and Ouabdesselam [10] have determined that 773 kJ/mole and 748 kJ/mole, respectively are the activation energies for the sintering of TiB_2. These high activation energies indicate that the

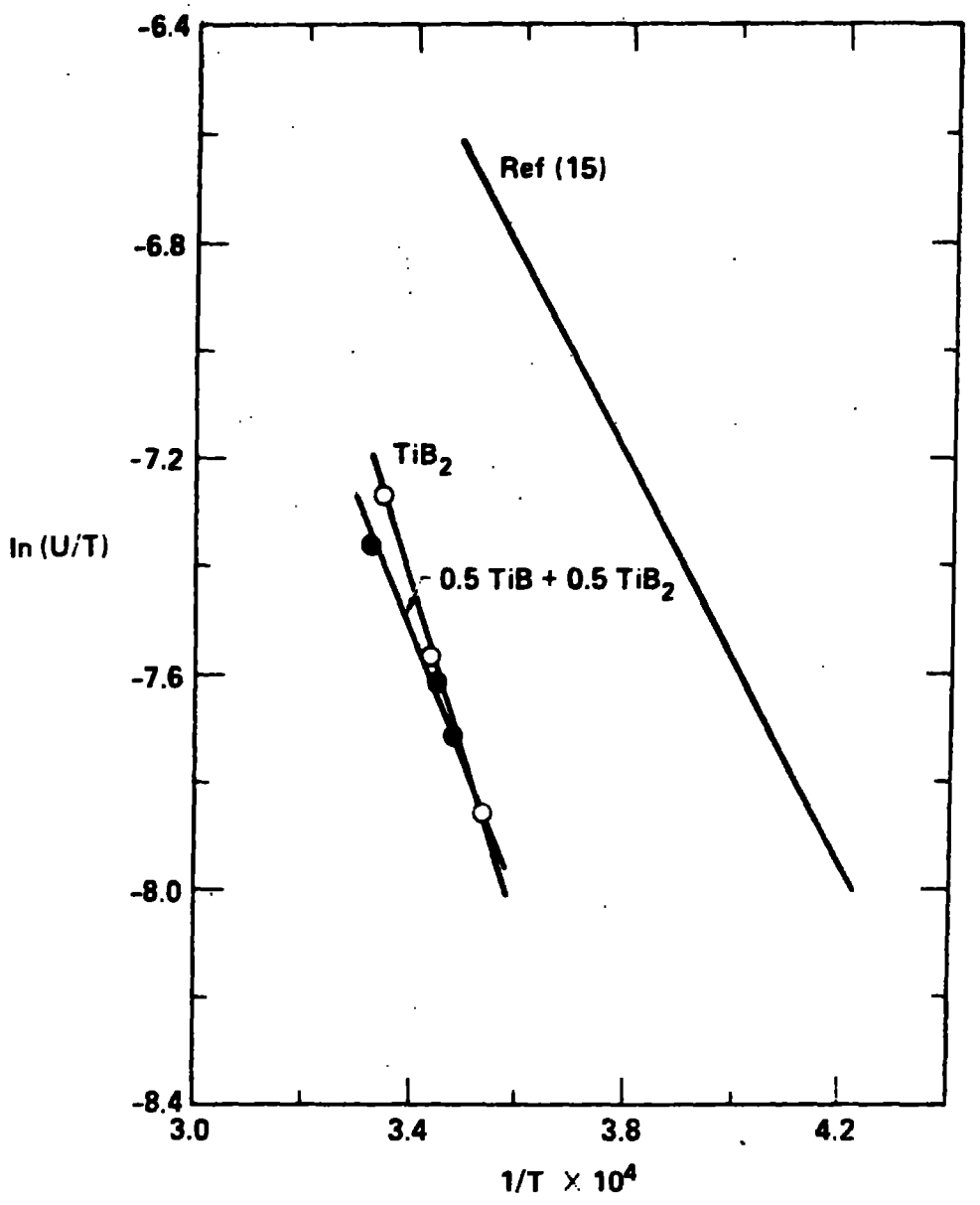

Fig. 2. Arshenius plots of the ln (u) versus VT for both the Ti-2B and Ti-1.5B compacts. Included is a line representing the data of Merzhanon [8].

mechanism for sintering is not the same as for combustion. So far as we know there is no self diffusion data of either Ti or B in TiB_2 for comparison. The reason for the large discrepancy between our results and these of Merzhanov are still unresolved. At corresponding temperatures, the velocities from [8] are in the 4-6 cm/sec range while our highest was 2.1 cm/sec. Their experiments were conducted under 10 atmospheres of argon while we used 1 atmosphere. The additional pressure may prevent the expansion of the compact during combustion. Another difference was our use of crystalline boron instead of amorphous boron. If their amorphous boron was smaller in particle size, then it should increase the velocity of combustion.

We also note that if calculated adiabatic temperatures in the combustion of Ti-2B are used instead of the measured temperatures, then we obtain an activation energy of 334 kJ/mole which is close to the Merzhanov value of 318 kJ/mole. As would be expected measured temperatures became closer to adiabatic conditions as the temperature is decreased. However, the Merzhanov paper [8] indicates that measured temperatures were used rather than the calculated values. Further study is necessary to provide answers for the difference in activation energies.

Equipment is being set up to measure the temperature profile of the combustion samples. This requires a rapid response data acquisition system with the capability to differentiate the curves. We plan to try both rapid response thermocouples and pyrometers for detecting the thermal signal. The activation energy may also be obtained from this data and will serve as an internal comparison to that obtained as outlined above.

TASK II. SIMULTANEOUS SYNTHESIS AND DENSIFICATION

INTRODUCTION

Compounds with large negative enthalpies of formation show correspondingly large contractions in volume from reactants to products. The large amount of porosity which is observed in the structure of most products of solid state combustion is partially the result of the difference in molar volumes between reactants and products. Figure 3 is a microphotograph of a polished section of a Ti-1.5B compact after combustion. The amount of porosity is near 50%. Another factor which contributes to the porosity of the combustion product is the original porosity of the reactant compact. This porosity prior to combustion may vary from 20 to 50%. In addition the expulsion of gases, such as water vapor which is adsorbed on the powders, may occur during combustion. These impurity gases may cause the expansion of the structure and introduce significant porosity.

For example, several compacts of Ti-1.5B were combusted in vacuum in order to identify the gases by mass spectrometry and determine their amount by pressure measurements. Listed in Table 3 is the gas analysis of a Ti-1.5B compact after combustion. The amount of gas evolved from a 5 g compact was 2.87×10^{-3} moles. Reference to Table 3 shows that 95% of the gas was hydrogen. The hydrogen could have come from that in solid solution in the titanium if it was processed in hydrogen or as a result of the dissociation of water vapor. If we assume that most of the hydrogen came from water vapor then it amounts to near 0.1% of the total sample weight.

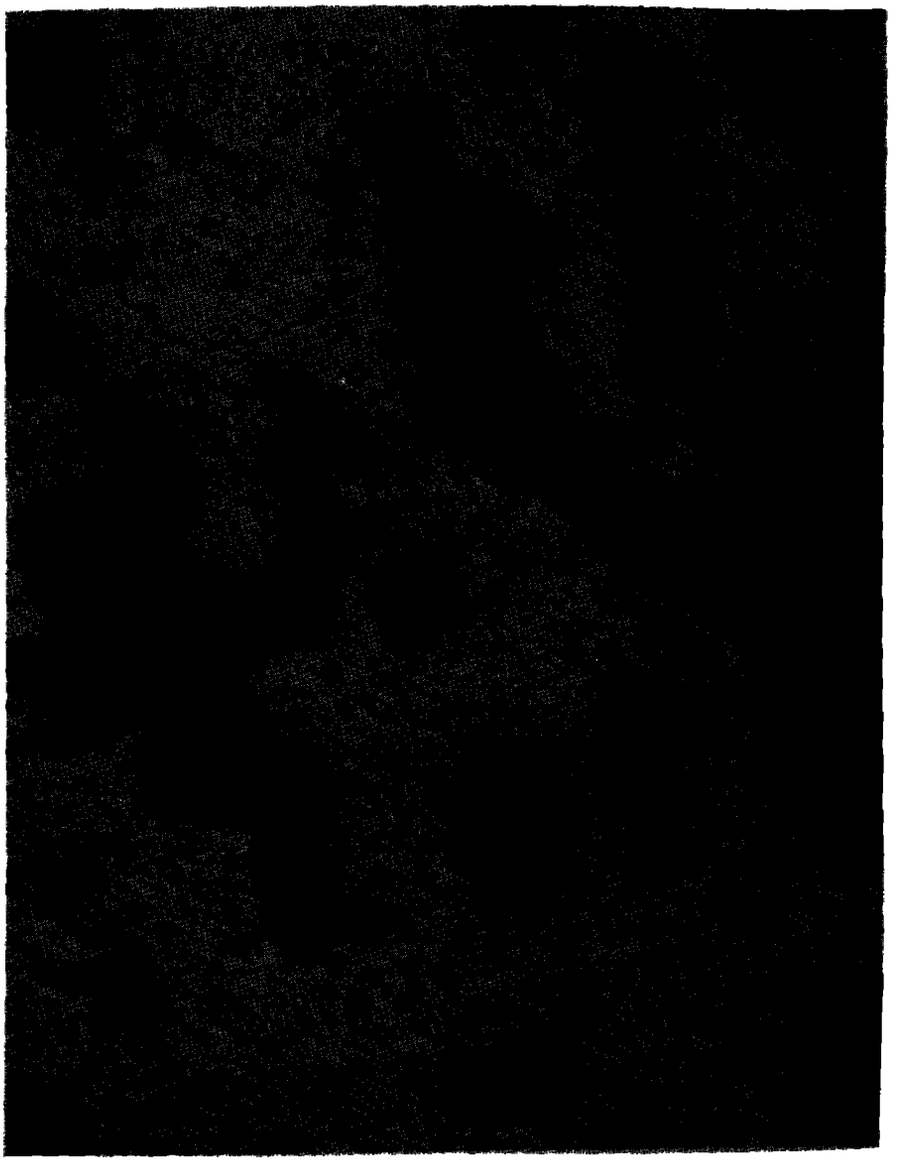

Fig. 3. Micrograph of polished section of Ti-1.5B compact after combustion. The section is a horizontal cut through the compact. The magnification is 200X.

TABLE 3. GAS ANALYSIS OF Ti-1.5B COMBUSTION

		Mole (Vol.%)
Nitrogen	N_2	4.509
Oxygen	O_2	0.017
Carbon Monoxide	CO	0.046
Hydrogen	H_2	95.28
Methane	CH_4	0.091
Ethane	C_2H_6	0.037
Propane	C_3H_8	0.012
		99.99

Total amount of gas evolved: 2.89×10^{-3} moles.

Since our objective is the simultaneous synthesis and densification of the combustion product then the different sources of porosity must be considered. Certainly, the most attractive method to accomplish densification would be through a chemical technique. For example, if a liquid phase is formed at the combustion front it may move through the compact with the formation of very little porosity. The liquid formation could be the result of the introduction of dopants into the reactants prior to combustion or the selection of a chemical system where the liquid layer at the front might naturally occur. In the Ti-2B system the adiabatic temperature (2965°C) is above the melting point of both titanium (1800°C) and boron (2300°C). Our experience with the combustion of Ti-2B shows, however, that the TiB_2 product is very porous with little indication of any densification.

ISOSTATIC PRESSURE

Other approaches to the problem of densification deal with the application of pressure either during or after combustion. We are investigating several techniques which combine high pressure with the combustion process. In previous work we demonstrated that TiC and TiB_2 compacts could be densified to 95%, and 97%, respectively of theoretical density. The reactant powders were rapidly heated in a graphite die (1200-1400°C/min) to the ignition temperature (1600-1800°C). Upon reaction the temperature rose very rapidly to near the melting point of the compound. Two thousand pounds of pressure was immediately applied to the hot material by graphite rams. If there was any pressure applied before or during reaction the die would be blown apart.

The use of high isostatic pressure appears to be a better procedure to produce densification during combustion. Three high pressure vessels are available for our densification experiments. The maximum pressure of each

vessel is 15,000 psi, 45,000 psi, and 200,000 psi, respectively. So far all of our work has been done in the 15,000 psi vessel. In order to determine the effect of the initial porosity several 98% dense Ti-2B compacts were formed by explosive compaction. One of these samples was burned without any external cladding at 15,000 psi. Since the TiB_2 product was still over 50% porosity, then the initial porosity is not a controlling factor in the densification process.

A variation of the high pressure experiment was to load Ti-2B powder into tantalum cans 1.9 in diameter and 2.5 cm in length. The lids were electron-beam welded onto the cans. Ignition of these samples by a tungsten coil was difficult. Because the highly viscous nitrogen gas transferred heat away from the top surface of the tantalum can. In later experiments the can was turned up-side down and insulated with fiber fax between the wall of the can and a outer quartz tube. In this configuration the sample could be ignited, but during the movement of the combustion wave the pressure in the contracting can exceeded the outside pressure causing the wall to burst. Several experiments have been conducted under similar conditions with the same results. These findings, along with the data from the outgassing during combustion experiments demonstrate that the adsorbed gases on the reactant powders are a serious deterrent to the densification process.

In cooperation with Mike Kelly of Mound Laboratory, plasma-formed Ti-2B compacts were prepared for combustion under high pressures. These compacts, 3-4 mm thick and 2.5 cm in diameter were 98-99% dense. Their method of fabrication should significantly reduce the amount of adsorbed gases on the powder reactants. Several attempts to ignite the compacts at atmospheric pressure were unsuccessful. Examination of a cross-section of one compact revealed a large excess of titanium which accounts for their non-ignition behavior. The process for fabrication of the compacts is being refined to form samples with the correct composition.

EXPLOSIVE COMPACTION

Another option for simultaneous synthesis and densification is to ignite reactants with a high pressure shock wave and compress the hot material in the same step. Highly exothermic powder reactants are known to have been ignited by shock waves [11]. The question to be answered is whether the shock wave can be used to densify the product. Our preliminary experiments were designed to show that Ti-2B powder could be ignited by shock waves generated from explosives. The latest fixture for these studies is shown in Fig. 4. Several modifications have been made to the fixture during a series of 15 shots. In one shot we did achieve ignition, however, the die blew apart and only a small amount of material was recovered. X-ray analysis of the material identified it as TiB_2. HMX at a density of about 1.33 g/cc has been used as the explosive. Pressures of about 150 kilobar have been produced in most of the experiments. Calculations have shown that 150 may be on the borderline for ignition, of the Ti-2B mixtures. For this reason our next shot using the fixture shown in Fig. 4 should generate pressures over 200 kilobars.

In all of these experiments the shock wave was used for ignition, but another concept is to ignite the sample in the usual way and then compress the hot material with a high pressure shock wave in the gas gun. The facilities for this type of experiment are being designed.

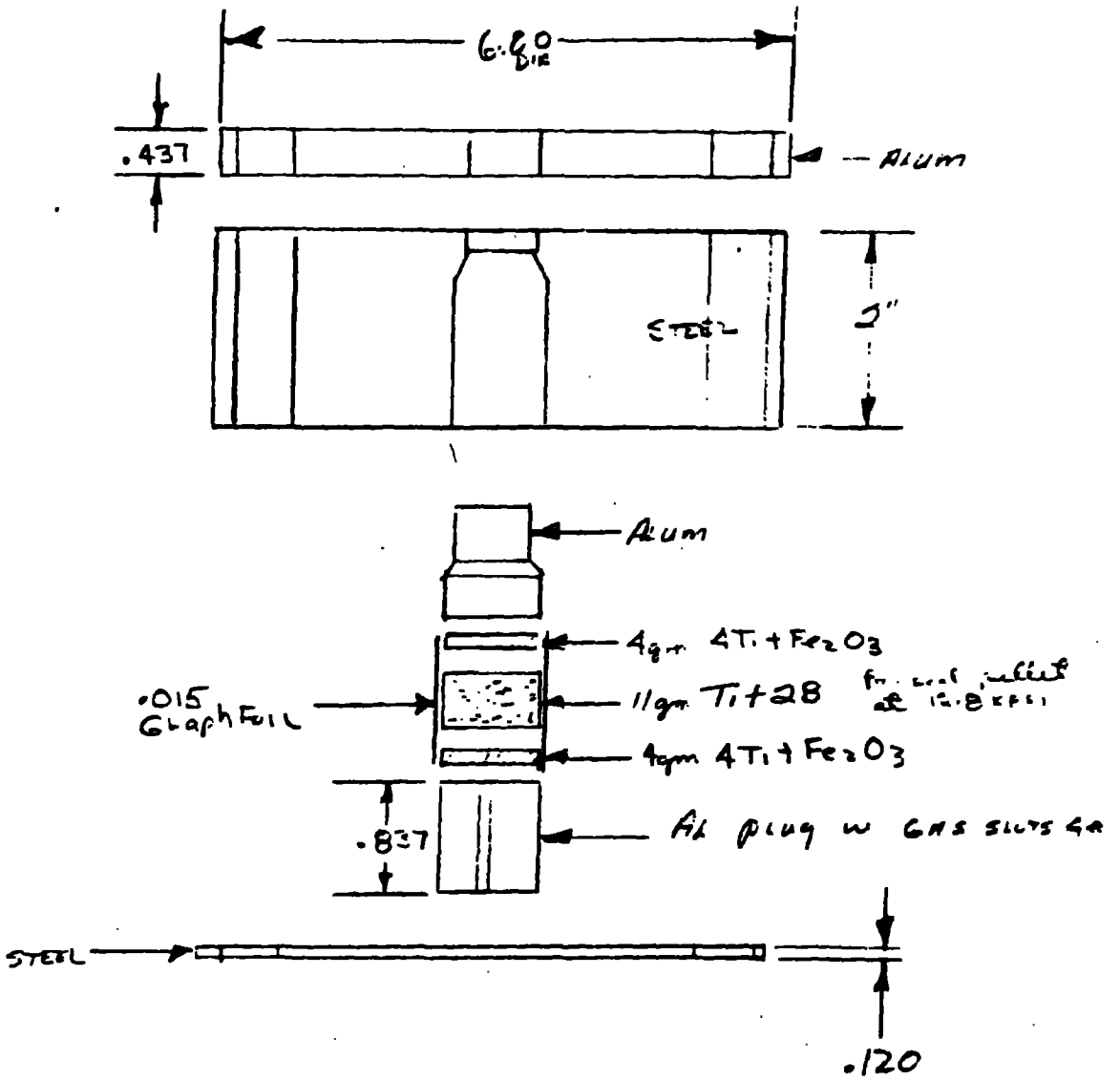

Fig. 4. A schematic drawing of the fixture used in the experiments to initiate and densify samples of Ti-2B using HMX explosive to supply the shock wave pressure.

REFERENCES

1. A. G. Merzhanov and I. P. Borovinskaya, Doklady Akad Nauk SSSR, Vol. 204, No. 2, pp. 366-369 May 1972.

2. A. G. Merzhanov and I. P. Borovinskaya, Combustion Science and Technology, Vol. 10, pp. 195-201, 1975.

3. N. P. Novikov, I. P. Borovinskaya, A. G. Merzhanov, Protesessy Goveniya v. Khimicheskoi Technologii I. Metallurgii, Chernogolovka, 1975.

4. A. G. Merzhanov, Archivum Combustionis, Vol. 1, No. 1/2, 1981.

5. A. G. Merzhanov, I. P. Borovinskaya, V. I. Yukhuid, and V. I. Ratnikov, Nauchnye Osnovy Materialovedeniia, Moscow, pp. 193-206, 1981.

6. A. G. Merzhanov, Archiwum Procesow Spalania, Vol. 5, No. 1, pp. 17-39, 1974.

7. T. S. Azatyan, V. M. Mal'tsev, A. G. Merzhanov, and V. A. Seleznev, Fizika Goreniya i Vzryva, Vol. 16, No. 2, pp. 37-42, 1980.

8. S. B. Margolis and B. J. Matkowsky, Combustion Science and Technology, pp. 193-213, 1982.

9. H. Pastor, Boron and Refractory Borides, Ed. V. I. Malkovich, p. 457, Springer-Verlag, 1977.

10. M. Ouabdesselem, University of California at Davis, Private Communication, 1984.

11. A. P. Hardt and R. H. Martinson, Proc. Eighth Symp. on Explosives and Pyrotechnics, The Franklin Research Center, Philadelphis, p. 53, 1974.

12. L. G. Raskolenko, Y. M. Maksimov, O. K. Lepakova, M. K. Ziadinov, and A. G. Merzhanov, Poroshkovaya Metallurgiya, No. 12 (204), pp. 8-13, 1979.

13. I. P. Borovinskaya, and V. E. Lorvaun, Dokl. Akad Nauk, USSR, Vol. 231, No. 4, p. 911-914, 1976.

14. V. K. Prokudina, T. V. Shestakova, I. P. Borovinskaya, I. G. Kuznetsova, N. A. Gracheva, and E. IE. Nedel'Ko, Problems of Combustion Technology; Materials of the third All-Union Conference on Technology of Combustion, 1981.

15. J. B. Holt and D. D. Kingman, Emergent Process Methods for High-Technology Ceramics, Materials Science Research, Vol. 17 Edited by Robert F. Davis, Hayne Palmour III and Richard L. Porter, p. 167, 1983.

SECTION II

J. Birch Holt
Lawrence Livermore National Laboratory

PLASMA CHEMICAL SYNTHESIS

INTRODUCTION

The objective of this research was to determine the feasibility of synthesizing fine AlN and Si_3N_4 with a nitrogen plasma. In this approach the plasma supplies one constituent of the compound. The metal powders are fed into the tail flame of the nitrogen plasma where they are vaporized. The boiling point temperature for Al and Si are 2057°C and 2600°C, respectively. The metal ions react with the nitrogen ions to form the nuclei of the nitride compound. To insure complete conversion NH_3 gas is directed into the tail flame. The distance of free fall influences the ultimate particle size of the final product. With AlN the particle size varies between 100Å to 500Å and in this case is controlled by the flow rate of NH_3. As expected the powder is highly agglomerated and is contaminated with approximately 7 wt% oxygen.

Synthesis of Si_3N_4 is more difficult because of the higher boiling point of the metal. The Si_3N_4 powder produced has been amorphous with approximately 200Å particles. In previous runs there has been some free silicon present in the amorphous powders. No attempt has been made to vary the particle size.

EXPERIMENTAL RESULTS

Our experimental runs have been designed to reduce the oxygen content of the fine powders of both AlN and Si_3N_4. We are convinced that nearly all the contamination is the result of our handling the powder in air. Consequently, chambers are being designed so that the synthesis and all subsequent handling will be done in an inert atmosphere. Our latest runs to form Si_3N_4 have been accomplished with smaller particle size silicon. In addition the feed mechanism has been improved so that a smoother flow of fine particles can be made into the plasma. The Si_3N_4 powder is now free of silicon. This latest powder must be characterized but it should be similar in size to previous powders.

In another series of runs we used SiO_2 powder rather than silicon to see if the oxide could be reduced in the nitrogen plasma. The results are inconclusive since the powder is amorphous to x-ray. SEM examination shows that some oxygen is still present which suggests we have an oxynitride material. The analysis of this powder has not been completed.

SECTION III

Prof. Zuhair A. Munir and K. A. Philpot
University of California, Davis

AN INVESTIGATION OF THE PRE-COMBUSTION PROCESS IN THE COMBUSTION SYNTHESIS OF Ni-Al COMPOUNDS

INTRODUCTION

Nickel and Aluminum react to form intermetallic compounds with large, negative enthalpies of formation, thus Ni-Al reactions exhibit self-propagating characteristics under the proper conditions.[1] The Ni-Al react to form four different intermetallic compounds. Also, at temperatures achieved during typical combustion reactions between Ni and Al, there is the potential for both solid-state reaction and liquid-state reaction. Study of Ni-Al combinations has the added advantage of the ability to work at relatively low temperatures. In comparison, temperatures achieved during combustion synthesis reactions involving carbides and borides are typically in excess of 2000°C.

The nickel-aluminum binary system was chosen as a model system for study of combustion synthesis reactions. By examining combustion synthesis reactions between Ni and Al, it has been the objective of this research to gain further insight into the mechanisms involved in these types of reactions and to better characterize the effects of pre-combustion processes on the actual combustion synthesis reactions.

SUMMARY OF RESULTS

This experimental study involved measuring T_i (the temperature at which the sample temperature first deviated from the furnace temperature) and δT (the difference between the maximum temperature measured during reaction and the baseline furnace temperature). Both parameters, shown in Fig. 1, were measured as functions of aluminum concentration, sample heating rate, and Ni powder particle size. As will be shown later, one or two exothermic peaks were recorded.

The composition range studied was from 5 - 30at% Al. Heating rates were varied from 0.5 to 5.0°C/min. Experiments were run on samples containing -200 mesh (<74μm). For practical purposes, average particle size was used for each size range when the data were plotted. Aluminum powder (-35 mesh i.e.,<43μm) was used as received for all experiments.

The dependence of T_i on the aluminum content of the alloy is shown in Fig. 2. There is a slight decrease in T_i for the first peak with Al concentration for both the 1 and 5°C/min heating rates. For the heating rate of 1°C/min, two temperature peaks were observed for Al concentrations up to 25at%. When the aluminum concentration was increased to 30at%, only one temperature peak was observed. In contrasts for the heating rate of 5°C/min, one temperature peak was observed for all Al concentrations.

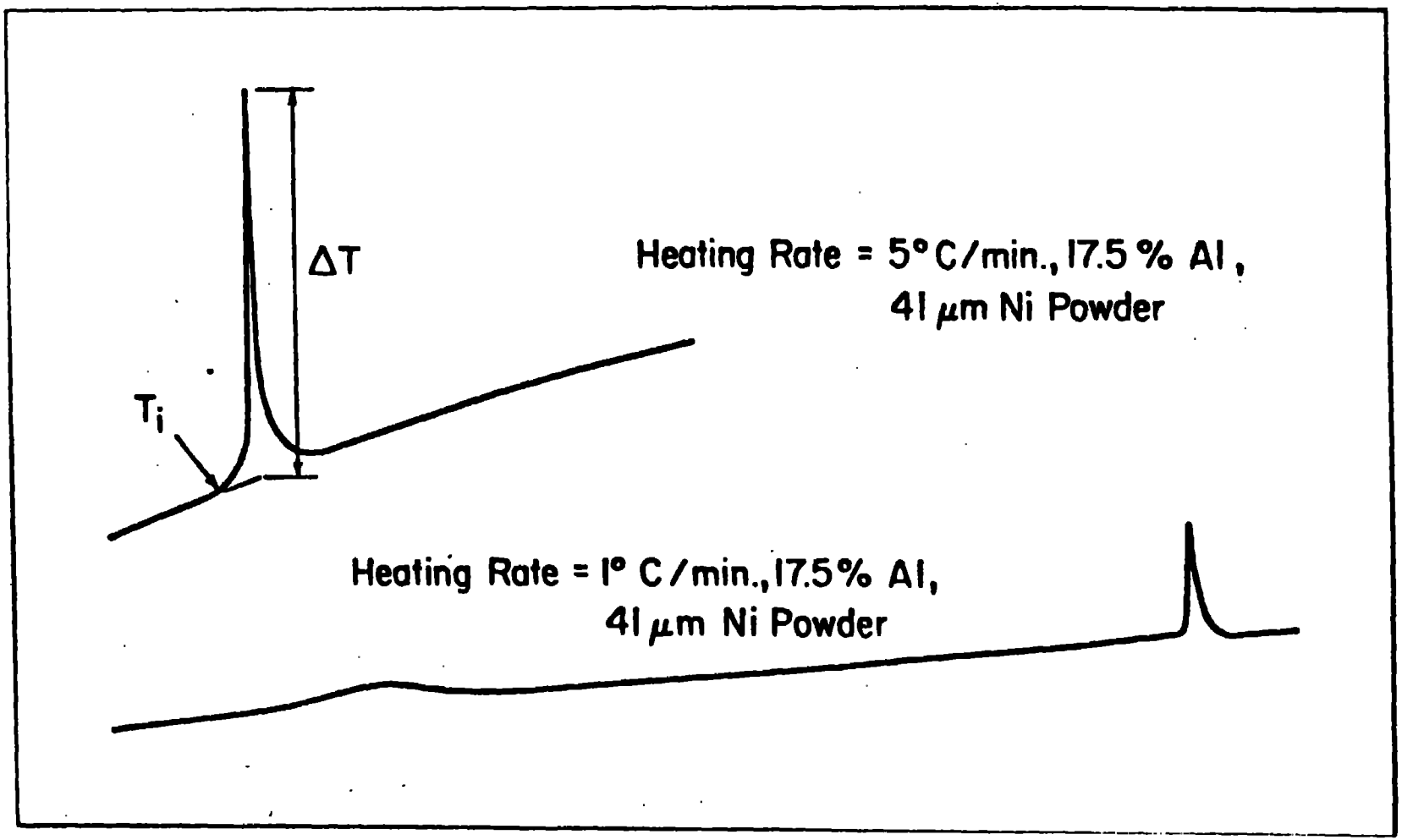

Fig. 1. Example of Temperature Peaks Observed Upon Reaction

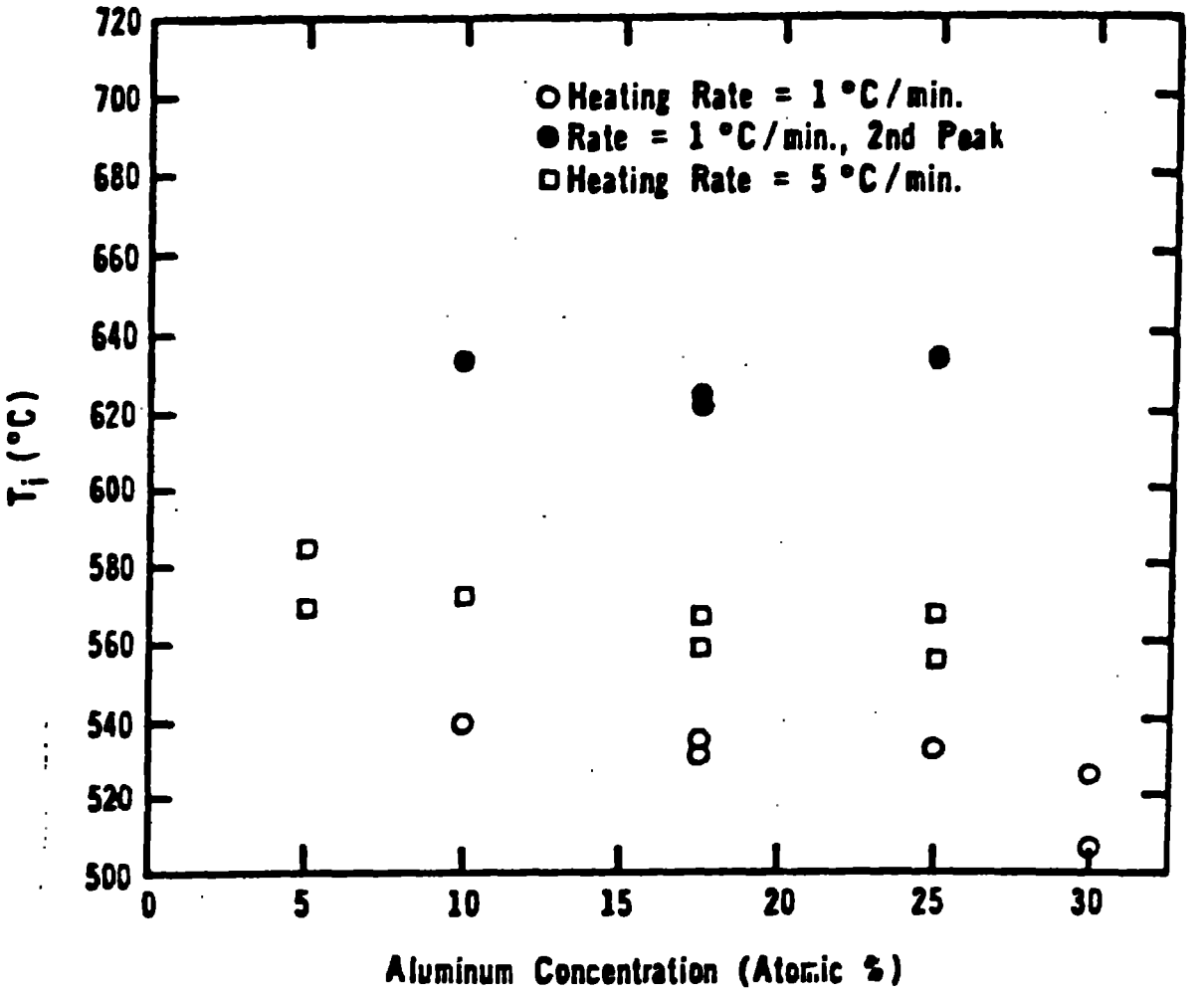

Fig. 2. The Variation of T_1 with Aluminum Concentration.

A plot of ΔT versus aluminum concentration is shown in Fig. 3 for heating rates of 1, 2, and 5°C/min. Also included in the plot are data obtained by Naiborodenko, et al.[2] for Ni-Al pellets made from Ni and Al powders which were both less than 50μm in size. The pellets reportedly contained 20% porosity.

The results show that ΔT increases dramatically with increases in aluminum concentration. It is interesting to note that in the case where both two peaks and one peak are observed for a given heating rate over the range of Al concentration (e.g., as in heating rate of 1°C/min) that the transition from two peaks to one peak is quite dramatic. In the case of heating rate of 1°C/min, from an Al concentration of 10 to 25at%, the increase in ΔT for both first peak and second peak is relatively small with increases in Al concentration. But when Al concentration is stepped up to 30at%, the observed ΔT value for the single peak increased to over 750°C.

The effect of heating rate on T_i is shown in Fig. 4 for samples containing 10 and 25at% Al. As can be seen from the plot, two peaks appeared for a heating rate of 1°C/min at both compositions. When the heating rate was doubled to 2°C/min, two peaks were observed only for samples with 10at% Al. At faster heating rates, only one peak was observed.

In Fig. 5 is shown the dependence of ΔT on heating rate. It is apparent that ΔT increases with increased heating rates. Also, at compositions of 17.5 and 25at% Al, Δt appears to reach an asymptotic value for heating rates above 2°C/min.

The transition in ΔT values from two peaks to one peak was sharp,especially at increased Al concentrations.

Experiments were run in which the size of the Ni powder was varied. As mentioned previously, the size fractions actually consisted of a range of particle sizes, but an average value was chosen for the purposes of plotting the data. The Al powder was -325 mesh (<43μ) for all experiments.

In Fig. 6 a plot of T_i versus nickel particle size is shown for specimens containing 10at% Al. Similar results (not included here) were obtained for 17.5 and 25at% Al. From Fig. 6, it appears that there is a trend of decreasing T_i with increasing Ni particle size for at least the first peak or the only peak where applicable. In general, two peaks were observed at lower heating rates and lesser Al concentrations as well as at larger particle sizes.

A plot of ΔT versus Ni particle size is shown in Fig. 7 for specimens with 10at% Al. Several trends were observed in these experimental results. In the case where two exothermic peaks were observed, ΔT for the first peak increased with decreasing Ni particle size. As ΔT increased in value for the first peak (i.e., with decreases in Ni particle size), ΔT for the second peak subsequently dropped in magnitude. At an average Ni particle size of 28μm, the ΔT value for the first peak was greater than ΔT for the second peak for samples of 17.5at% Al, heated at 1°C/min and 10at% Al, heated at 2°C/min.

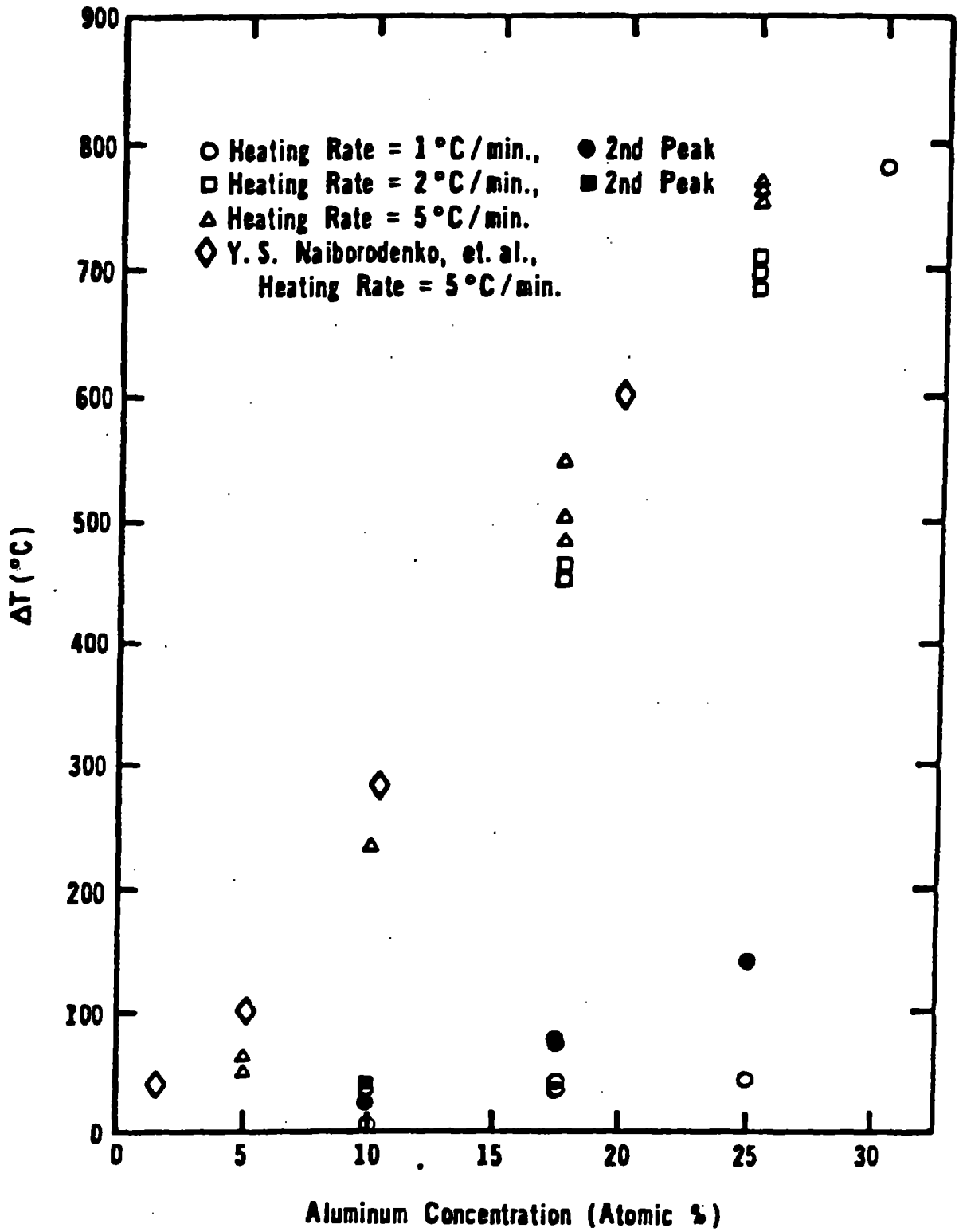

Fig. 3. The Variation of ΔT with Aluminum Concentration.

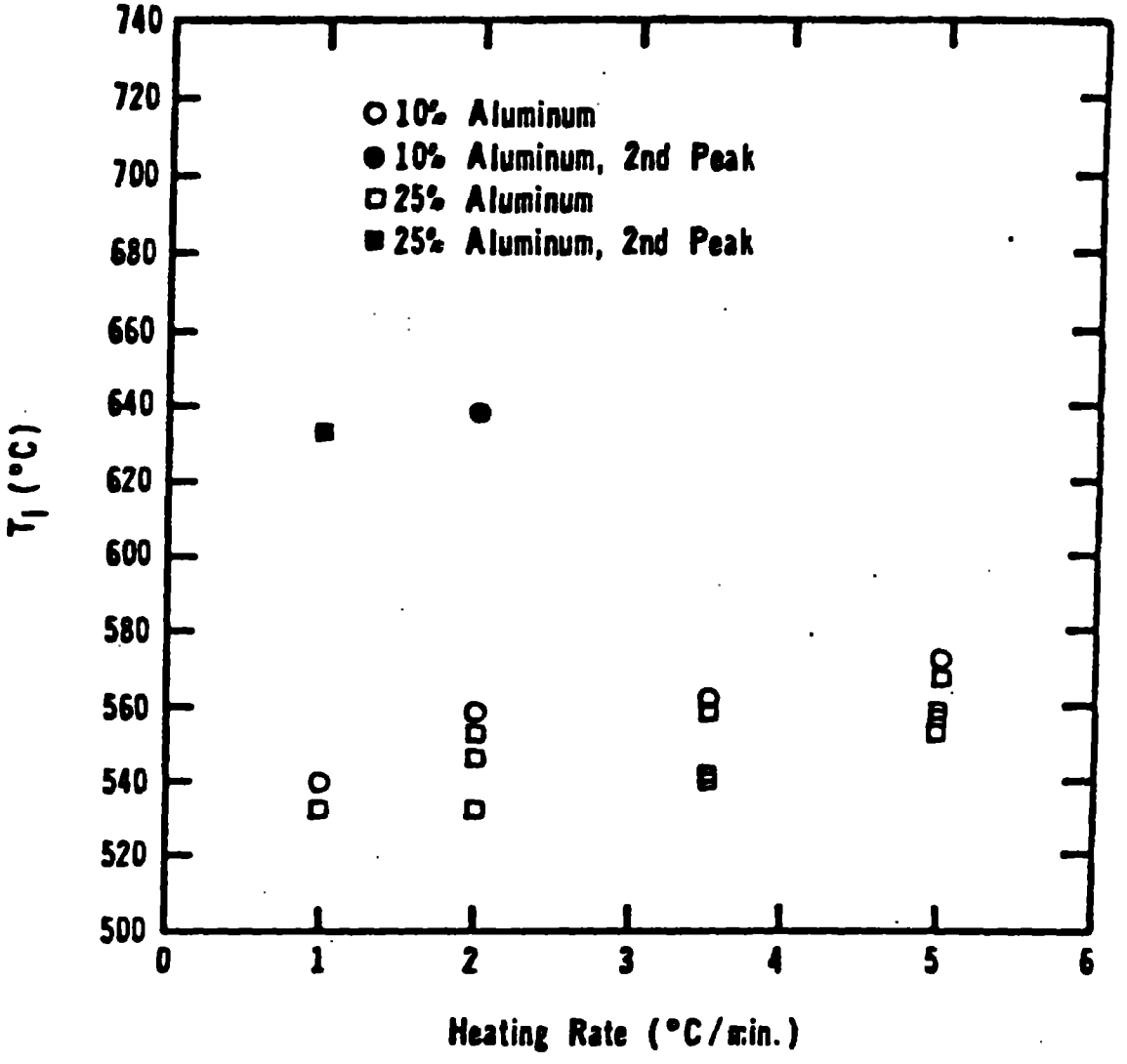

Fig. 4. The Effect of Heating Rate on T_1.

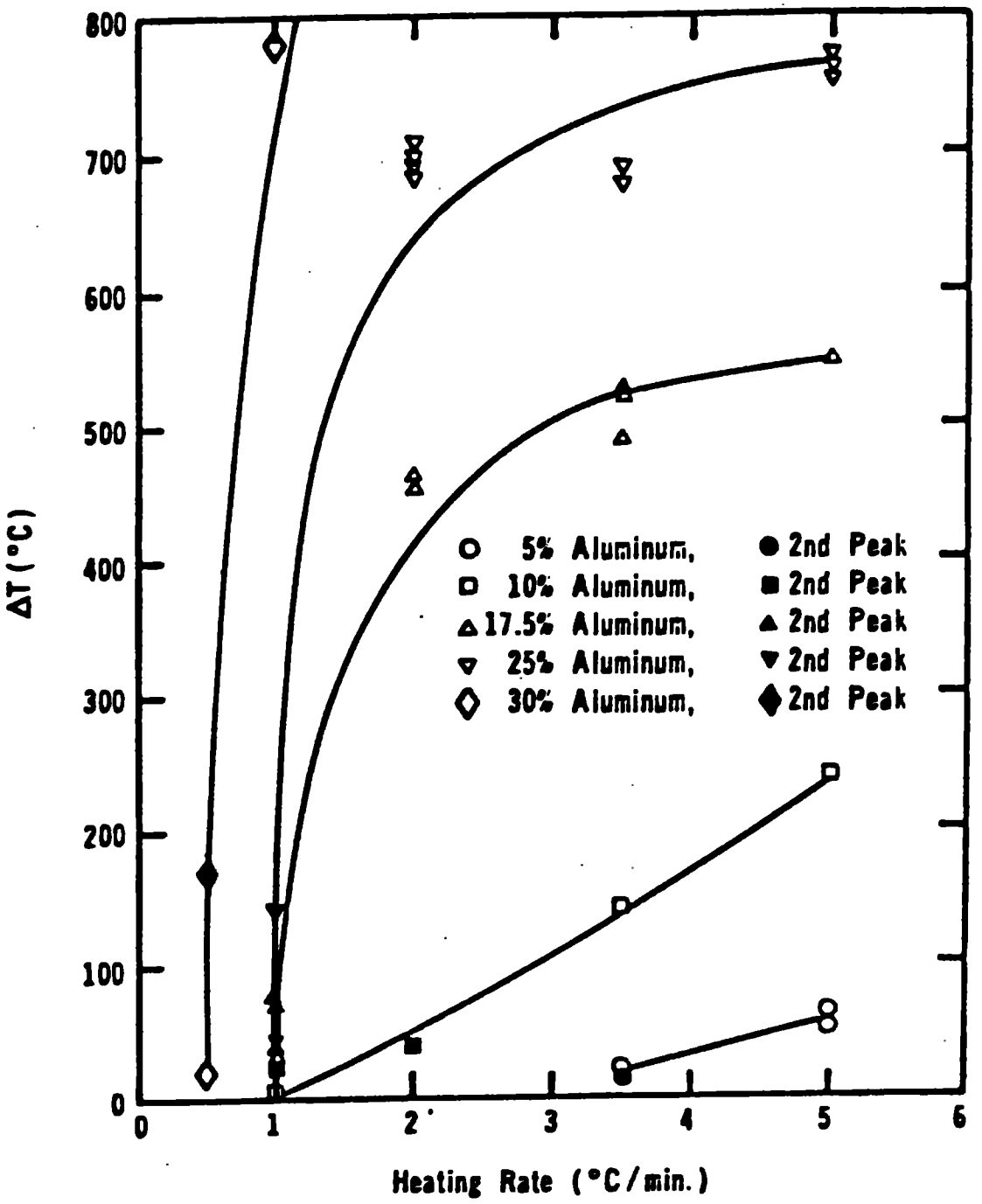

Fig. 5. The Effect of Heating Rate on ΔT.

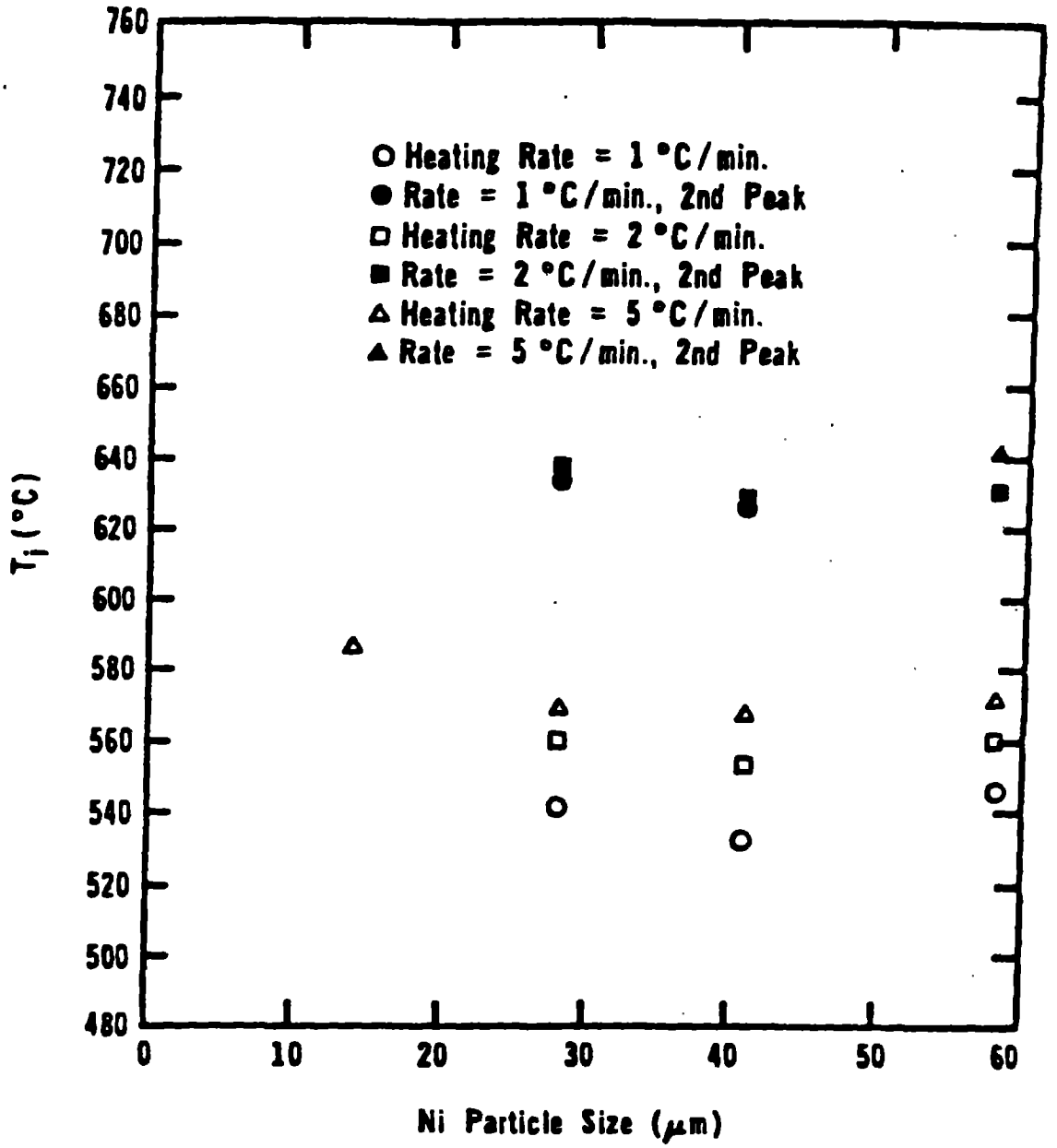

Fig. 6. The Effect of Ni Particle Size on T_i for 10at% Al Samples.

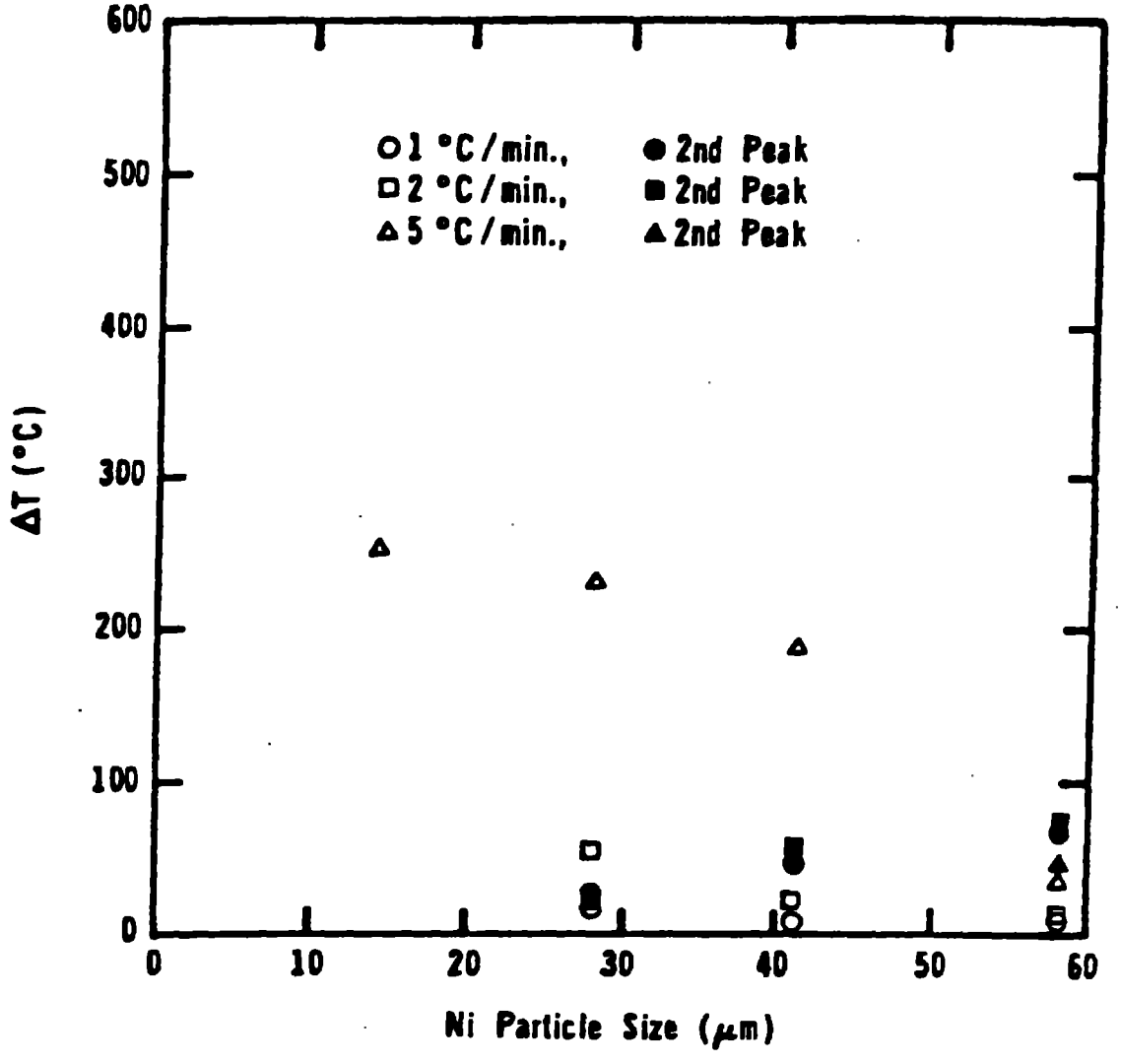

Fig. 7. The Effect of Ni Particle Size on ΔT for 10at% Al Samples.

In the case where one exothermic peak was observed, ΔT increased with decreases in Ni particle size. As observed preciously, the transition from two peaks to one peak was dramatic, particularly for higher Al concentrations.

CONCLUSIONS

For Ni-Al mixtures in the range of 5-30at% Al, it was found that the major compound that ultimately forms was $AlNi_3$. When the compacts were heated slowly ($\sim$1°C/min), $AlNi_3$ formed to a large extent in the solid state through a series of reactions where Al_3Ni and Al_3Ni_2 formed initially. $AlNi_3$ then forms by a reaction involving Ni and Al_3Ni_2 and most likely AlNi. When the sample temperature reaches 640°C, and remaining Al melts and quickly reacts with Ni to form more $AlNi_3$.

When the samples are heated rapidly, not much solid-state reaction takes place, though it is known that the solid-state reaction serves to initiate the rapid, liquid-solid reaction. In this case the $AlNi_3$ that forms is primarily from a reaction between Al in the melt and Ni. Because the enthalpy of formation of $AlNi_3$ from Al and Ni is greater than that for forming $AlNi_3$ from AlNi and Ni, much larger ΔT values are observed at increased heating rates. It was also noted that intermetallic compound formation did not always result in a detectable temperature peak. X-ray diffraction analysis showed that Al_3Ni and Al_3Ni_2 formed in the solid state at temperatures as low as 500°C which was below the temperature of the first peak at slow heating rates. Also, it was found that $AlNi_3$ formation occurs (at slow heating rates) between the temperatures where the first and second peak are observed, with no apparent rise in sample temperature.

In conclusion, this study of exothermic reactions between Ni and Al has shown the complexities involved in reactions of this type. Solid-state reaction plays a strong role, even at increased heating rates. The types of products that were formed were found to be related to not only the rat at which the sample was heated and the chemical composition of the sample, but also to the size of the powders used in the mixture.

REFERENCES

1. Y.S. Naiborodenko, V.I. Itin, A.G. Merzhanov,I. P. Borovinskaya, V.P. Ushakov, and V. P. Maslov, Sov. Phys. J., 16, 872 (1973).

2. Y.S. Naiborodenko, V.I. Itin, B.P. Belozerow, and V.P. Ushakov, Sov. Phys. J., 16, 1507 (1973).

SECTION IV

Raymond A. Cutler
Ceramatec, Inc.

COMBUSTION SYNTHESIS OF THERMITE-REACTIONS

RESEARCH OBJECTIVE

To gain a better understanding of parameters affecting the synthesis of oxides and carbides made by exothermic reactions. The synthesis of silicon carbide powder and its sinterability is of particular interest. The major emphasis of this work is do use submicron oxides and carbon as starting materials in order to synthesize submicron powders.

PROGRESS THIS QUARTER

At the program review in Houston (February 5-6, 1985) progress was reported on determining the effect of SiO_2, Mg, and C size on the surface area of the resulting powder synthesized by the following reaction:

$$SiO_2 + 2\ MG + C \rightarrow SiC + 2\ MGO \qquad (1)$$

Table 1 lists the compositions of the first series (coded "series 4") of powders prepared, as well as a second set (coded "series 20") of powders which are more deficient in carbon. The compositions coded with the letters A-G (i.e., 4A-G) are identical except for the particle size of the carbon (or graphite) used. Compositions H and I have 0.1-0.3 micron diameter SiO_2 substituted for the 0.008 micron diameter silica used in the other compositions. Compositions J and K have -60, +100 mesh Mg instead of -325 mesh magnesium, code M uses colloidal graphite, and code L powders have no carbon added in order to compare the following reaction with Reaction (1):

$$SiO_2 + 2MG \rightarrow Si + 2MgO \qquad (2)$$

Table 2 gives the surface area of the reacted powders prepared by Reactions (1) and (2) for all of the "series 4" powders as well as the "series 20" powders. The "series 4" powders were synthesized under bacuum as loose powders wrapped in graphite foil. Figure 1 shows the effect of initial carbon surface area on the surface area of powder synthesized by Reaction (1), as reported at the Houston meeting. Table 2 clearly shows that undesired phases (Mg_2Si, Si and C) were observed to different degrees in all of the powders. Figure 2 is an x-ray diffraction (XRD) pattern of code 4K powder showing Mg, Mg_2Si, and Si in addition to MgO and SiC. Figure 3 is an XRD pattern of the same powder after acid leaching in HCl and HF. Figure 3 shows that some free graphite exists in the powder. The surface area of the leached 4K was 87.6 $\pm$ 0.8 m^2/g, indicating that some free carbon is in the acid washed powder. Likewise the surface areas of acid washed 4C, 4D, 4F, 4H, 4I, 4J, 4L and 4M powders were 48.4, 155.5 79.8, 49.6, 51.0 105.7 30.3, and 86.3 m^2/g (standard deviations were 1 - 3 m^2/g), respectively. The level of carbon additions for the "series 4" powders was determined based on weight loss in argon. In order to avoid free carbon in the reacted powders, the "series 20" powders were made based on the percent volatiles given by the manufacturer.

TABLE 1. COMPOSITION OF REACTANTS

Code	Composition (weight grams)			Carbon Type	
	SiO_2[a]	Mg[b]	C	Tradename	Surface[c] Area (m^2/g)
4A	63.53	48.62	14.59	Raven 40-220[d]	1075
4B	63.53	48.62	14.71	Raven 7000[d]	625
4C	63.53	48.62	14.11	Raven 3500[d]	320
4D	63.53	48.62	12.85	Raven 1020[d]	95
4E	63.53	48.62	12.34	Raven 410[d]	25
4F	63.53	48.62	12.19	Gulf A.B.[e]	65
4G	63.53	48.62	12.07	Micro 880[f]	9
4H	60.07[g]	48.62	12.19	Gulf A.B.[e]	65
4I	60.17[h]	48.62	12.19	Gulf A.B.[e]	65
4J	63.53	48.62[i]	14.59	Raven 40-220[d]	1075
4K	63.53	48.62[i]	12.19	Gulf A.B.[e]	65
4L	63.53	48.62	-	-	-
4M	63.53	48.62	60.00	DAG 154[j]	-
20A	60.70	48.62	12.19	Raven 40-220[d]	1075
20B	60.70	48.62	12.90	Raven 7000[d]	625
20C	60.70	48.62	12.46	Raven 3500[d]	320
20D	60.70	48.62	12.18	Raven 1020[d]	95
20E	60.70	48.62	12.08	Raven 410[d]	25
20F	60.70	48.62	12.00	Gulf A.B.[e]	65
20G	60.70	48.62	12.00	Micro 880[f]	9
20H	60.07[g]	48.62	12.00	Gulf A.B.[e]	65
20I	60.17[h]	48.62	12.00	Gulf A.B.[e]	65
20J	60.70	48.62[i]	12.19	Raven 40-220[d]	1075
20K	60.70	48.62[i]	12.00	Gulf A.B.[e]	65
20L	60.70	48.62[i]	-	-	-
20M	60.70	48.62	60.00	DAG 154[j]	-

[a] Fumed silica (Cab-O-Sil HS-5 (325 ± 25M^2/G)), Cabot Corp. (Boston, MA) unless otherwise indicted.

[b] Magnesium (MG-203 (-325 mesh)), Atlantic Equipment Engineers (Bergenfield, NJ) unless otherwise indicted.

[c] Surface area (B.E.T. method) as determined by manufacturer.

[d] Columbian Chemical Co. (Tulsa, OK).

[e] Gulf Acetylene Black, Gulf Oil Chemicals Co. Baytown, TX).

[f] Graphine, Asbury Graphite Mills, Inc. (Asbury, NJ).

[g] SI-238 (-325 mesh), Atlantic Equipment Engineers.

[h] SI-239 (-325 mesh), Atlantic Equipment Engineers.

[i] MG-130 (-60, + 100 mesh), Atlantic Equipment Engineers.

[j] Collodial graphie (20% solids in isopropanal) Acheson Colloids Co. Port Huron, MI).

TABLE 2. CHARACTERIZATION OF REACTED POWDERS

Code	Initiation Temperature[a] °C	B.E.T. Surface Area (m^2/g)			X-ray Diffraction Intensity Relative to MgO (220)			
		#[b]	x[c]	s[d]	β -SiC (111)	Si (111)	Mg_2Si (220)	C
4A	557	2	20.02	1.53	28	5	8	0
4B	556	2	18.68	0.29	24	7	8	0
4C	580	3	17.72	0.48	28	6	8	0
4D	551	3	7.49	0.42	23	17	11	0
4E	562	3	3.38	0.16	27	38	17	0
4F	565	3	9.36	0.64	27	40	18	0
4G	567	3	4.13	0.11	23	42	27	20
4H	608	3	11.76	1.15	0	28	57	59
4I	598	3	10.98	0.32	0	38	28	66
4J	674	3	33.24	0.31	24	12	10	0
4K	630	3	8.31	1.10	30	34	11	0
4L	555	2	1.58	0.15	0	40	84	0
4M	545	3	4.90	0.03	27	0	8	0
20A	597[e]	f	f	f	33	16	40	0
20A	572[g]	f	f	f	34	28	72	0
20A	525	f	f	f	33	44	32	0
20A	590[e,h]	f	f	f	42	5	11	0
20B	559[e]	f	f	f	29	7	16	0
20E	559[e]	f	f	f	19	6	19	0
20G	535	f	f	f	11	24	47	18
20H	537	f	f	f	f	f	f	f
20I	532	f	f	f	f	f	f	f
20J	667[e]	f	f	f	f	f	f	f
20K	589	f	f	f	f	f	f	f

[a] Reacted as loose powder in vacuum unless otherwise noted.

[b] Number of samples analyzed.

[c] Mean value.

[d] Standard deviation

[e] Reacted after isostatically pressing at 207 MPa (30 ksi).

[f] Work in progress.

[g] Reacted after isostatically pressing at 34.5 MPa (5 ksi).

[h] Reacted in one atmosphere Ar.

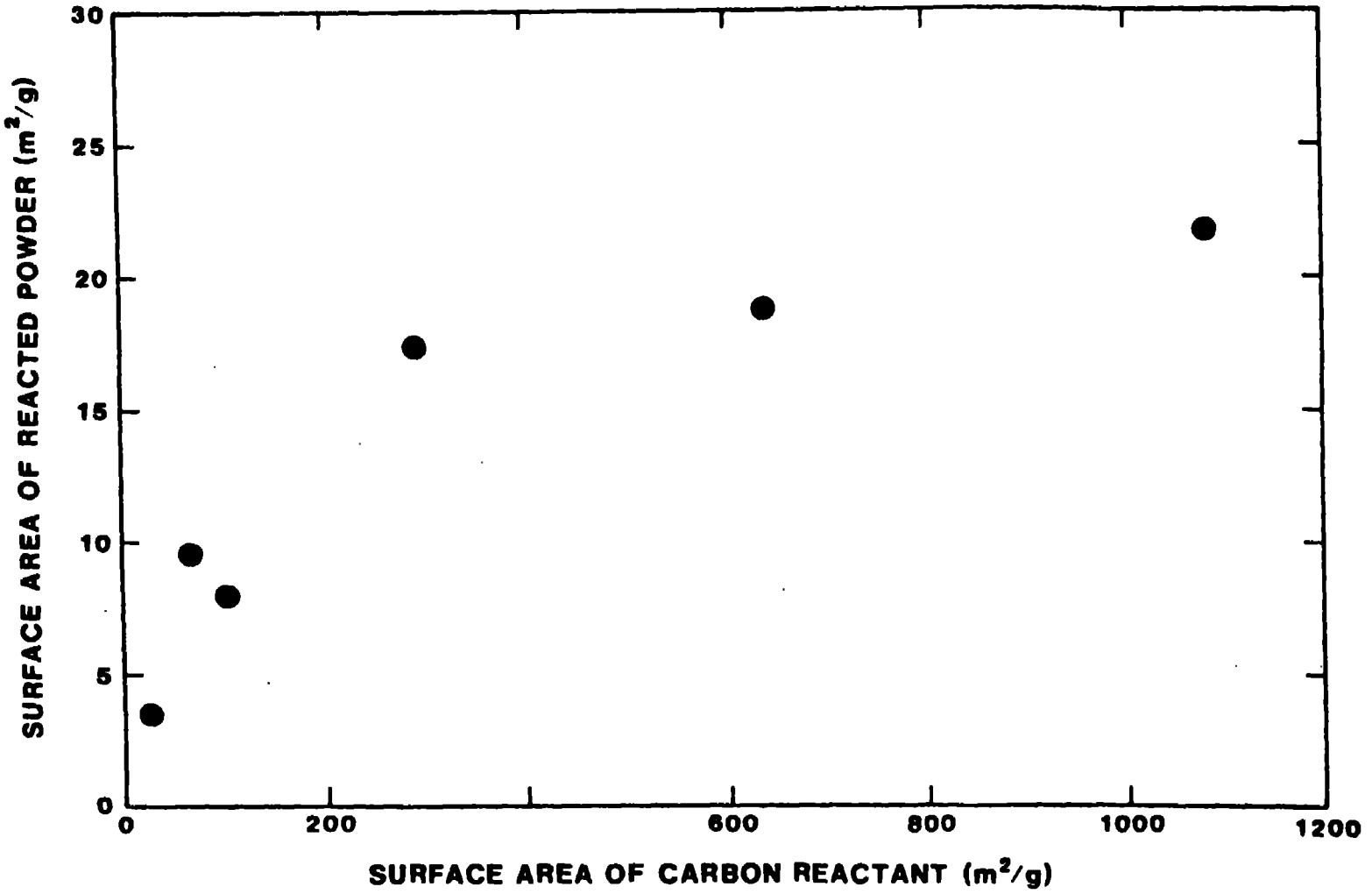

Fig. 1. Effect of initial carbon surface area on the surface area of powder synthesized by Reaction (1)

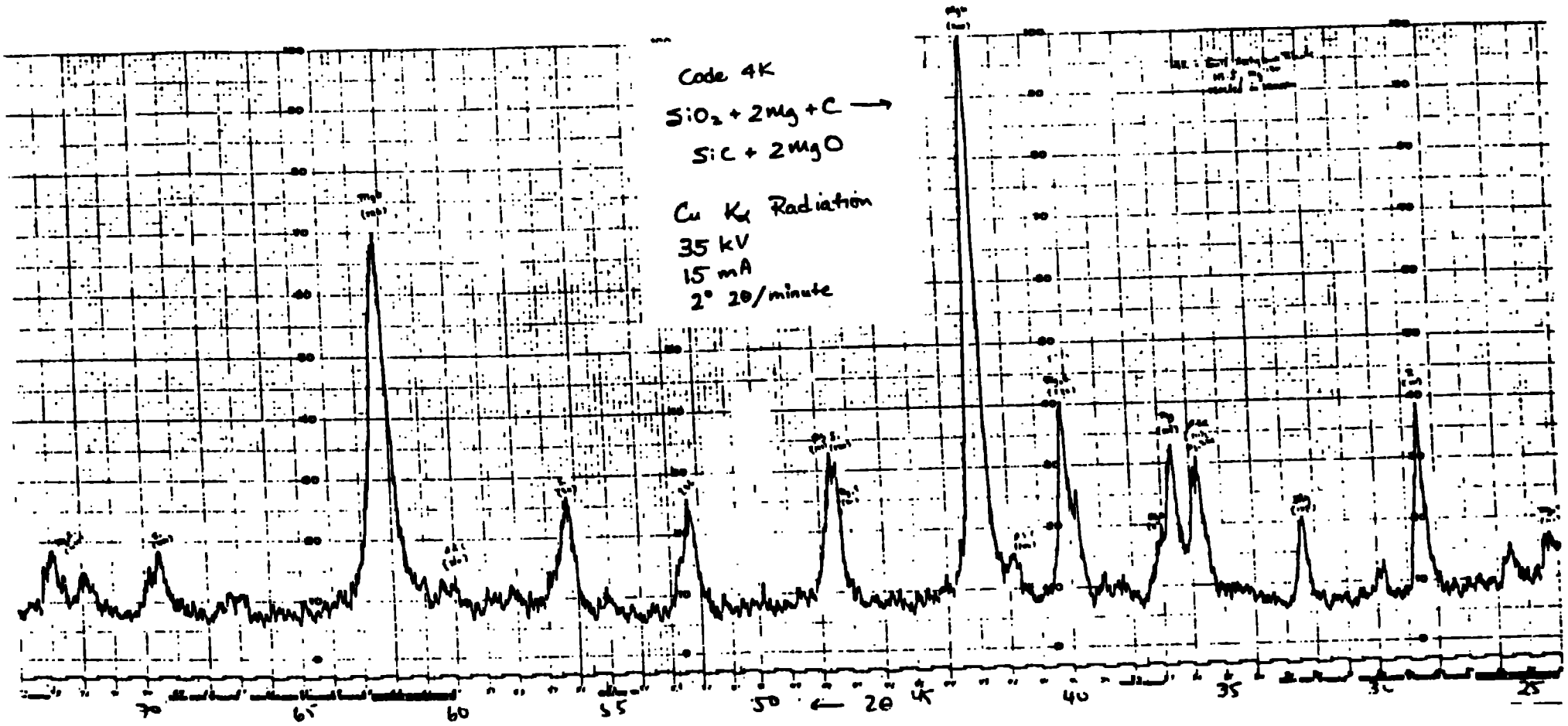

Fig. 2. X-ray diffraction pattern of Code 4K (See Tables 1 & 2) reacted in vacuum. Note that Mg_2Si, Mg and Si are evident in the reacted powder.

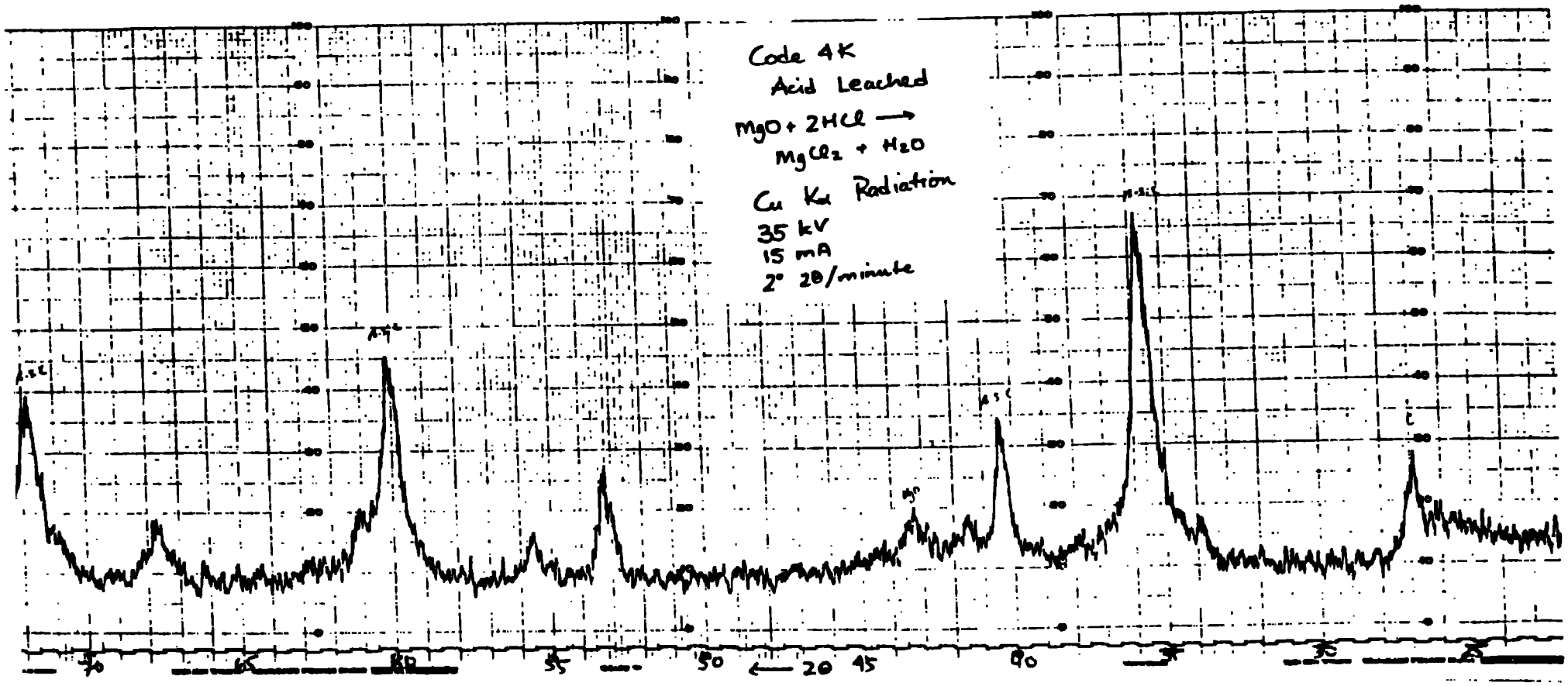

Fig. 3. X-ray diffraction pattern of Code 4K after acid leaching in HCl and HF. Some graphite and MgO were detected by XRD.

Despite the problems in determining surface area, the SEM photomicrographs in Fig. 4 clearly reconfirms that Reaction (1) is a viable approach for making submicron SiC powders. The mean particle size of the acid leached 4F powder is 0.10 to 0.15 microns. Further characterization of the acid leached powders is planned using TEM.

In addition to lowering the carbon content in the "series 20" powders, it was also desired to retain more of the powder in the graphite foil after sintering. Series 20 powders were generally compacted to 207 MPa (30 ksi) isostatically before igniting. In order to see the effect of powder compaction on initiation temperature and the particle size of the reacted powders, code 20A powders pressed at 207 MPa were compared with the same powder precompacted at 34.5 MPa, and loose powder. The initiation temperature increased with compaction pressure (see Table 2) despite the fact that uniform heating was used to initiate the reaction. The amount of SiC was qualitatively the same based on XRD but the amount of free Si decreased with increasing pre-compaction pressure (see Table 2). The yield of reacted powder in the graphite foil increased dramatically, as did the overall yield of powder from within the tube furnace. All three reacted powders were easily crushed in a mortar and pestal. Further characterization by surface area and SEM is in progress to determine what effects the precompaction had on the particle size and degree of agglomeration of the reacted powders.

The effect of atmosphere is clearly visible when comparing 20A powders reacted in vacuum with the same powder reacted in one atmosphere argon. The initiation temperatures are identical, but the powder reacted in argon had much lower Mg, Si, and Mg_2Si than the powder reacted in vacuum (compare Figs. 5 and 6). This is in agreement with previous work by the principal investigator which showed that XRD patterns free of intermetallics or free Si or Mg were possible by reacting in Ar. Further experimentation in Ar and N_2 will follow characterization of the "series 20" powders. It is currently believed that carbon control in vacuum will eliminate the presence of undesired phases.

Several observations are possible based on the powders reacted to date: (1) Surface area measurements on reacted and acid washed powders show that Mg particle size does not influence the particle size of the synthesized powders (compare powder 4F with 4K or 4A with 4J in Table 2). The higher initiation temperature of the coarser Mg has been verified by the "series 20" experiments. The higher initiation temperature is believed to be related to the lower Mg vapor pressure caused by the decreased surface area of the larger particles; (2) Carbon particle size appears to influence the particle size of the reacted powders, although further characterization of the powders is required before a firm conclusion can be drawn; and (3) the silica particle size is very important as evidenced by the lack of SiC formation for powders containing coarser SiO_2 (compare 4H and 4I with 4F). For both series of powders the reactions involving coarser silica were detected by the vacuum pump (gases evolved during the reaction) rather than the brilliant light evolved during most reactions. The H and I powders, in both cases, had only a faint glow at the time of the reaction. Alternative silica sources will be investigated, as well as other gas environments in order to determine the range of SiO_2 particles sizes where Reaction (1) will go to completion.

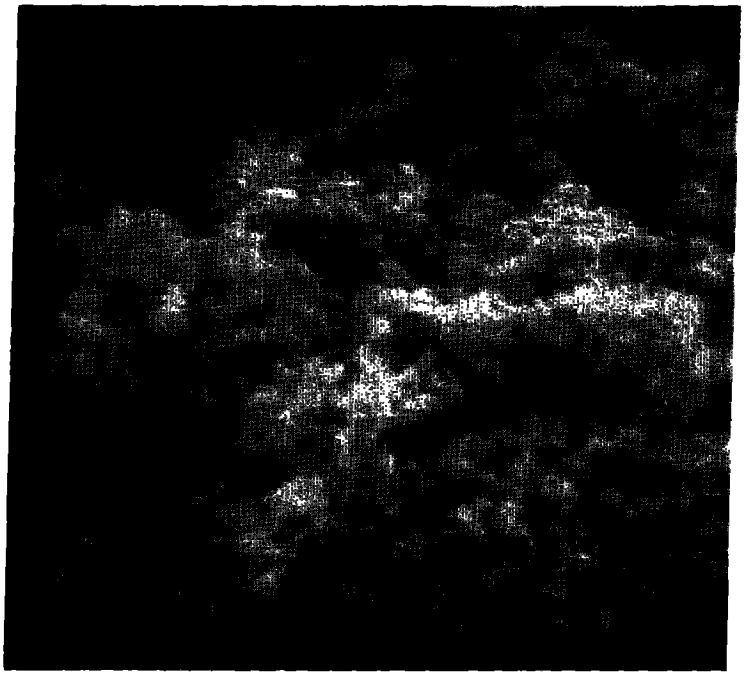

(a)

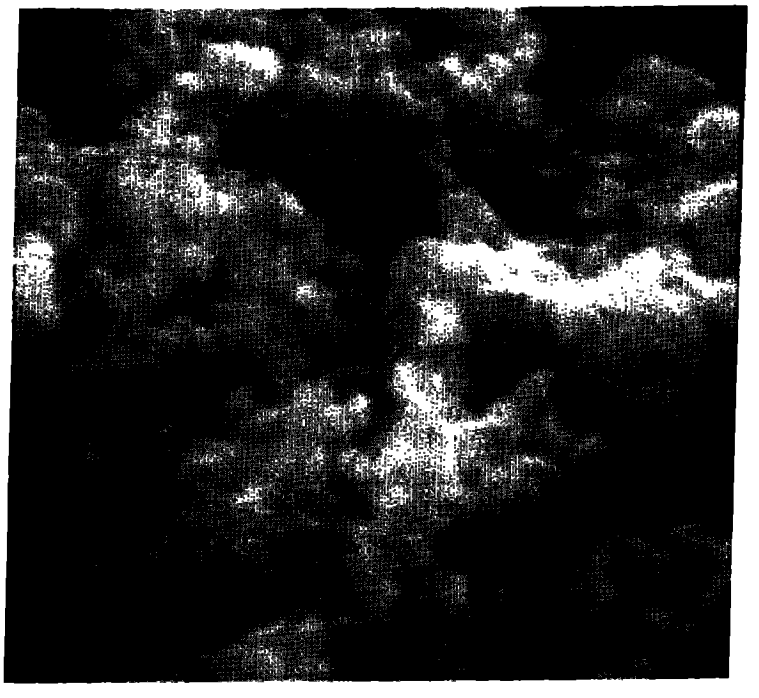

(b)

Fig. 4. SEM photomicrographs showing submicron SiC powder synthesized by Reaction (1). Powder is acid leached 4F. (a) 20,000X, (b) 40,000X.

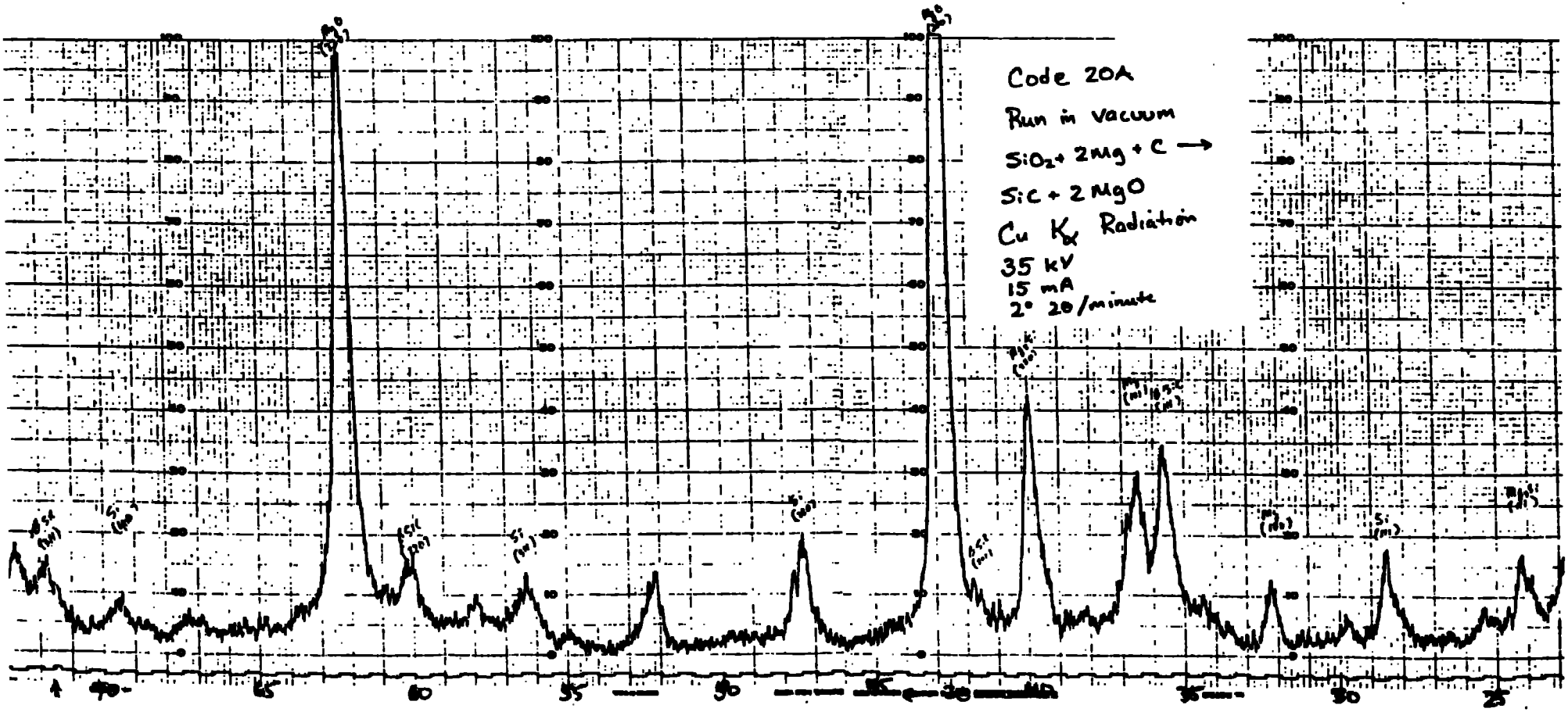

Figure 5. XRD pattern of 20A powder (precompressed to 207 MPa) reacted in vacuum. Compare with Figure 6.

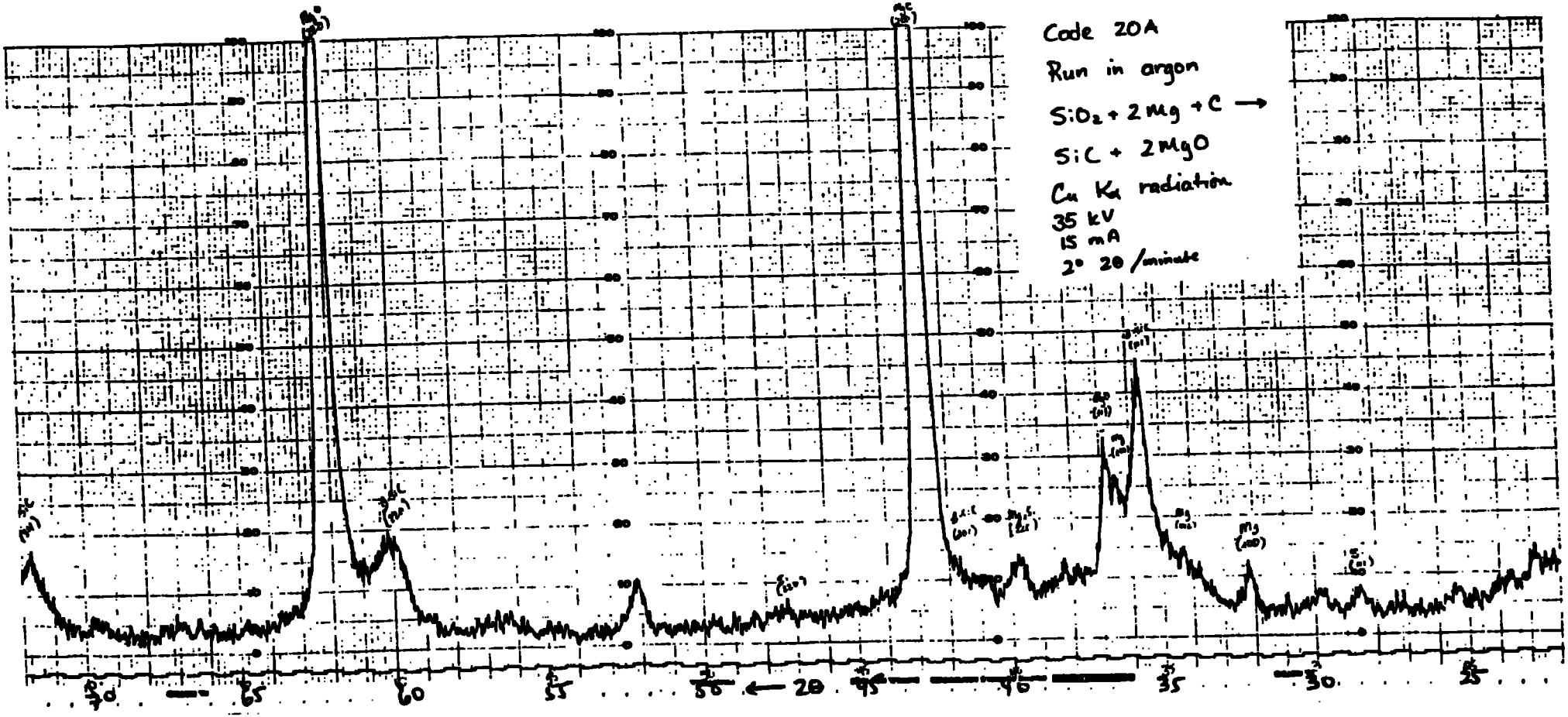

Figure 6. XRD pattern of 20A powder (precompacted to 207 MPa) reacted in argon. Note that Si, Mg_2Si and Mg peaks are much smaller than in powder reacted in vacuum (see Figure 5).

While the feasibility of synthesizing submicron powders from submicron oxide and carbon reactants has clearly been demonstrated, the principal investigator is not aware of any work in which submicron compounds were synthesized by self-combustion synthesis of elements. This may be due to different transport mechanisms for diffusion or it may simply be due to the fact that researchers are using larger carbon or graphite than that used in the present investigation. In order to further clarify the effect of initial carbon particle size on the reacted product, experiments using the following reaction were initiated:

$$TiH_2 + C \rightarrow TiC + H_2 \qquad (3)$$

Titanium hydride was chosen over titanium metal due to the brittleness of the hydride allowing its particle size to be reduced during milling, thus providing a more intimate mixture. The powders listed in Table 3 were milled for 30 minutes in a stainless steel mill using WC-Co media. The air dried powers were pre-compacted to 207 MPa isostatically. Heating of the powders to 475°C for one hour in Ar was used to reduce the hydride to the metal. The samples were then reacted by Dr. Holt at LLNL using an ignitor, since heating rates are not fast enough to initiate the reaction (TiC formed during heating) using the experimental set-up at Ceramatec.

The surface areas of the reacted powders (Table 3) indicated that the carbon particle size (see Table 1 for the surface area of the carbon powders) affected the surface area of the SHS synthesized TiC. Particle size determinations at LLNL by sedimentation indicated that the agglomerate sizes were all over 5 microns. Scanning electron microscopy was therefore used to characterize the reacted pellets. Figure 7 shows clear evidence of melting for code 21A powder (see Table 3), indicating that the adiabatic temperature was reached. The TiC particle were as small as 0.7 50 1.2 microns prior to melting. Figure 8 shows that while code 21B TiC had also melted in most areas (see Figs. 8a and 8b), there were some unmelted grains (Fig. 8c) and areas were the grain size was still fine (0.8 microns) despite partial melting (see Fig. 8d). Code 21D, the powder with the largest starting particle size, also had the largest grain size (Fig. 9a shows 12.7 micron diameter agglomerate). Code 21E TiC 1 (Figs. 9b, 9c, and 9d) was also fused with some areas of local sintering.

While this set of experiments showed the same trend as Reaction (1) powders (see Fig. 1), it was also inconclusive due to the melting of the TiC. Further experiments will be performed over the summer using diluents to lower the temperature of Reaction (3) as well as substituting Ta for Ti, since TaC will not melt. It is currently felt that while carbon (or boron or nitrogen) particle size can be used to make submicron carbides (or borides or nitrides) by SHS synthesis, the use of submicron oxides is a much more effective method for synthesizing submicron materials.

Limited experiments were performed using the following reactions:

$$3SiO_2 + 4Al + 3C \rightarrow 3SiC + 2Al_2O_3 \qquad (4)$$

$$3TiO_2 + 4Al + 3C \rightarrow 3\ TiC + 2\ Al_2O_3 \qquad (5)$$

TABLE 3. CHARACTERIZATION OF SHS POWDERS

Code[a]	Composition (weight (grams))			Reacted Powder Surface Area	Calculated Particle
	TiH_2	C	C Source[a]	m^2/g)	Size[b](μm)
21A	100.00	24.38	Raven 40-220	2.19	0.28
21B	100.00	24.92	Raven 3500	1.62	0.38
21C	100.00	24.16	Raven 410	0.91	0.67
21D	100.00	24.00	Asbury 880	0.10	5.96
21E	100.00	24.00	Gulf A.B.	0.66	0.92

The purpose of the aluminothermic reduction of silica was to see if intermetallics were evident when reactions were carried out in vacuum in this system (previous results had shown that experimentation in N_2 or Ar showed no evidence of intermetallics or free Al or Si). Additionally, it was desired to compare a waste product (Elkem's microsilica) with the high purity fumed silica (see Table 4). XRD of the two powders were very similar (compare Figs. 10 and 11) with stronger peaks evident with microsilica powder (23A) than fumed silica (23B). Both powders were very friable after the reaction. Characterization of these powders are limited to date, but samples will be sent to AMMRC in order to see if the exothermic reaction purified the 94-98% microsilica in comparison to the 99.9% fumed SiO_2. The x-ray data did show some free Si and experiments will be performed in Ar in order to verify that atmosphere affects Reaction (4).

Similarly, Reaction (5) was carried out to determine if intermetallics or free Ti are formed. Additionally, it was desired to see if Al_2O_3-30 wt. % TiC powders could be formed by adding the appropriate amount of Al_2O_3 filler during the reaction. Previous experiments had shown that cutting tools made by milling powders made by Reaction (5) with alumina had comparable properties to composites made by milling conventionally prepared powders. Code 23C results in 30 wt. % TiC, code 23D in 40 wt. % TiC, and 23E in 46.7 % TiC (code 23E is based on the stoichiometry shown in Reaction (5)).

Code 23C powder was heated to 687°C before the reaction initiated and the reaction time was approximately five seconds. The 207 MPa precompressed cylinder was partially sintered and very difficult to crush. As shown in Fig. 12, the only phases present were alumina and titanium carbide. SEM photomicrographs (see Fig. 13) show that the particle size varies from 0.05 to 0.5 microns with a mean particle size near 0.3 microns. There is no evidence of melting and some sintering of particles has occurred. The starting carbon particle size in Fig. 13 is identical to that in Figs. 9a-9c. It has conclusively been shown that both the alumina and titanium carbide are submicron. Further experimentation will show the utility of using this approach to make cutting tools. Additionally, the addition of an alumina diluent to powder 21E will allow a comparison to be made between Reactions (3) and (5). Code 23D powder ignited at 643°C and showed the same XRD pattern as code 23C. Instead of staying in one mass, however, the precompacted powder was observed to be in thin plate-shaped sections after the reaction. The reaction time was also much faster (less than one second) as expected. Further characterization of Reaction (5) powders is underway.

(a)

(b)

Fig. 7. SEM photomicrographs of TiC (Code 21A) prepared using Raven 40-220 Carbon ($1075 m^2/g$). Note that TiC is fused together. TiC particle size is as small as 0.7 to 1.2 μm (4000X).

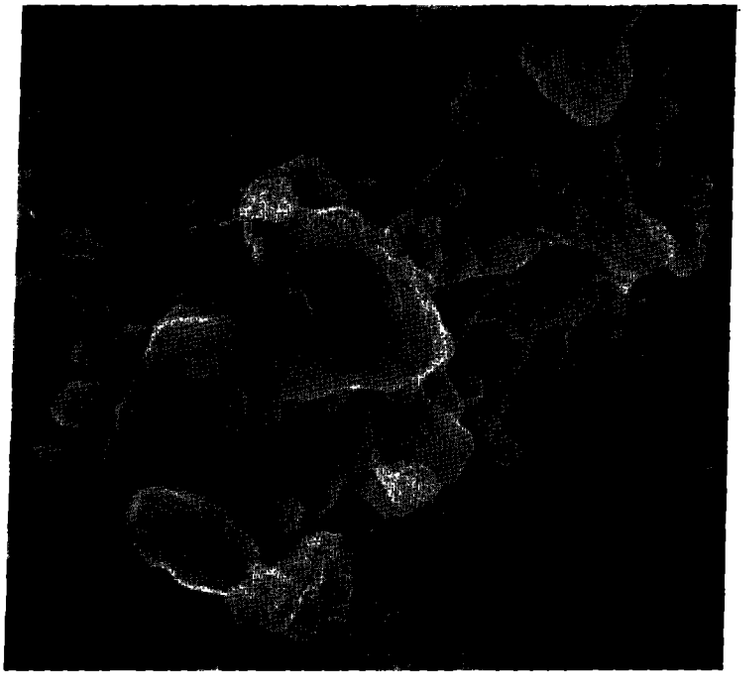

(a)

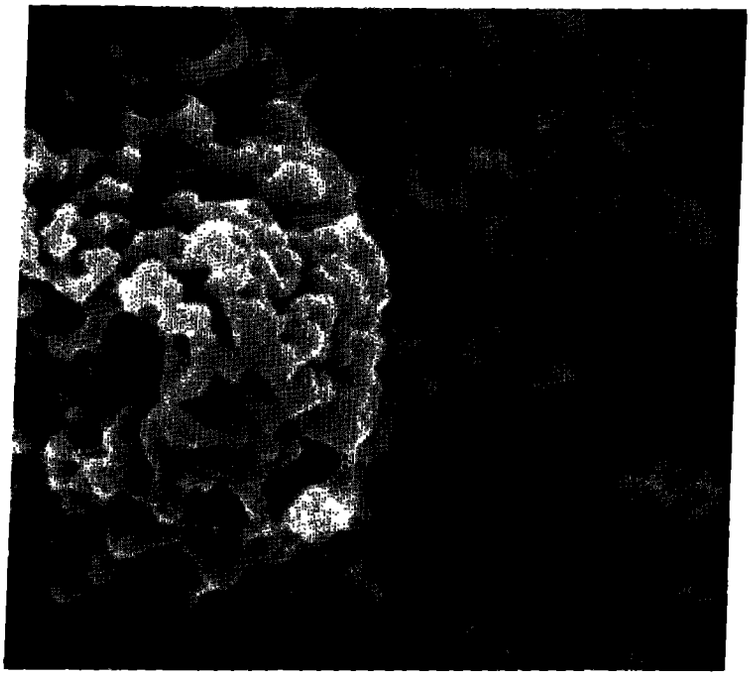

(b)

Fig. 8. SEM photomicrographs of TiC (21B) prepared using Raven 3500 carbon ($320 m^2/g$). (a) Fused particles (4000X), (b) fused particles which are as small as 1.6 μm (4000X).

(c)

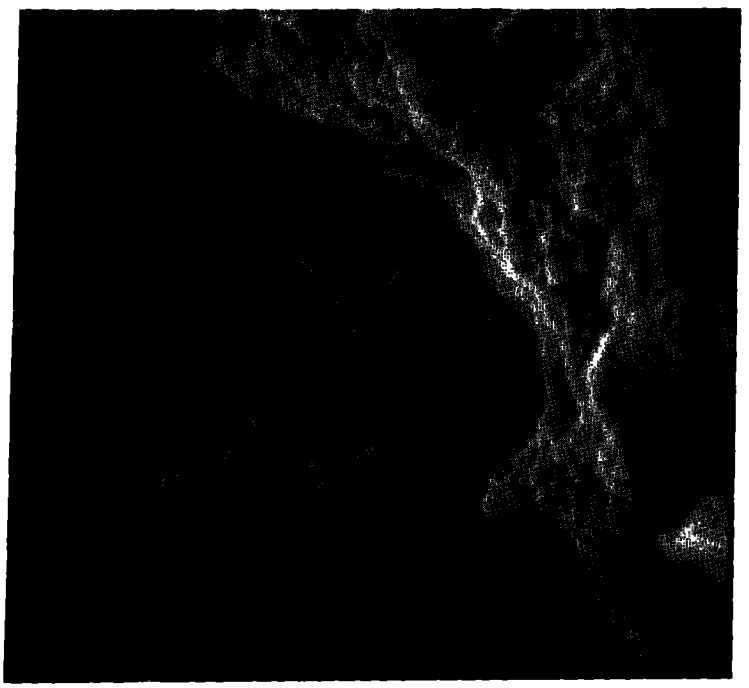

(d)

Fig. 8. (cont.) (c) Crystalline TiC grains which are approximately 4.5 μm in diameter (7800X), and (d) fused TiC grains as small as 0.6 μm in diameter (4000X).

(a)

(b)

Fig. 9. TiC prepared by Reaction (3). (a) Code 21B ($9 m^2/g$ graphite). Agglomerate size is 12.7 μm (6000X). (b) Code 21E ($65 \mu m^2/g$ acetylene black) showing fused TiC (4000X).

(c)

(d)

Fig. 9. (cont.) (c) Code 21E showing areas of local sintering (400X), and (d) Code 21E showing fused surface (4000X).

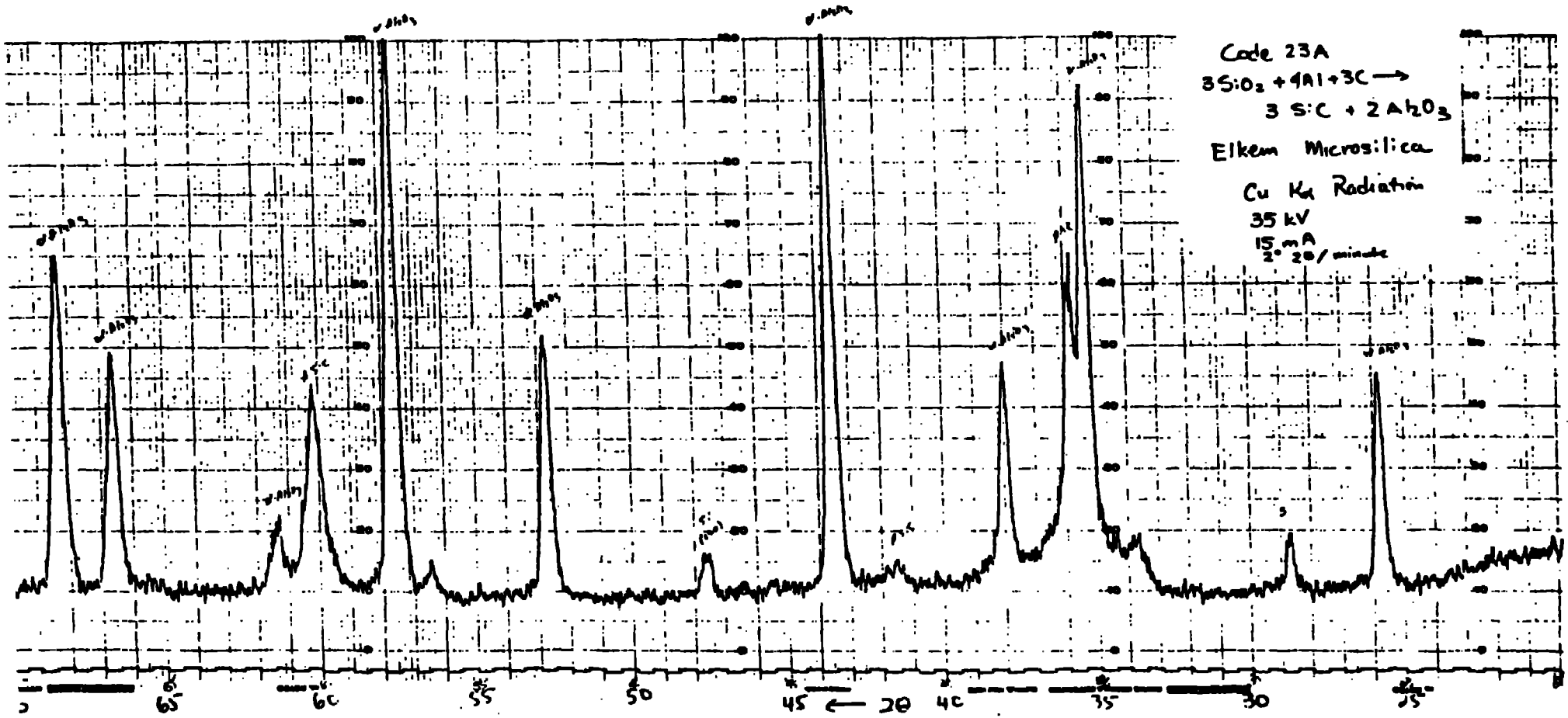

Fig. 10. XRD pattern for $SiC-Al_2O_3$ powder prepared by Reaction (4). A low purity silica (Code 23A in Table 4) was used to make the SiC. Compare with Figure 11.

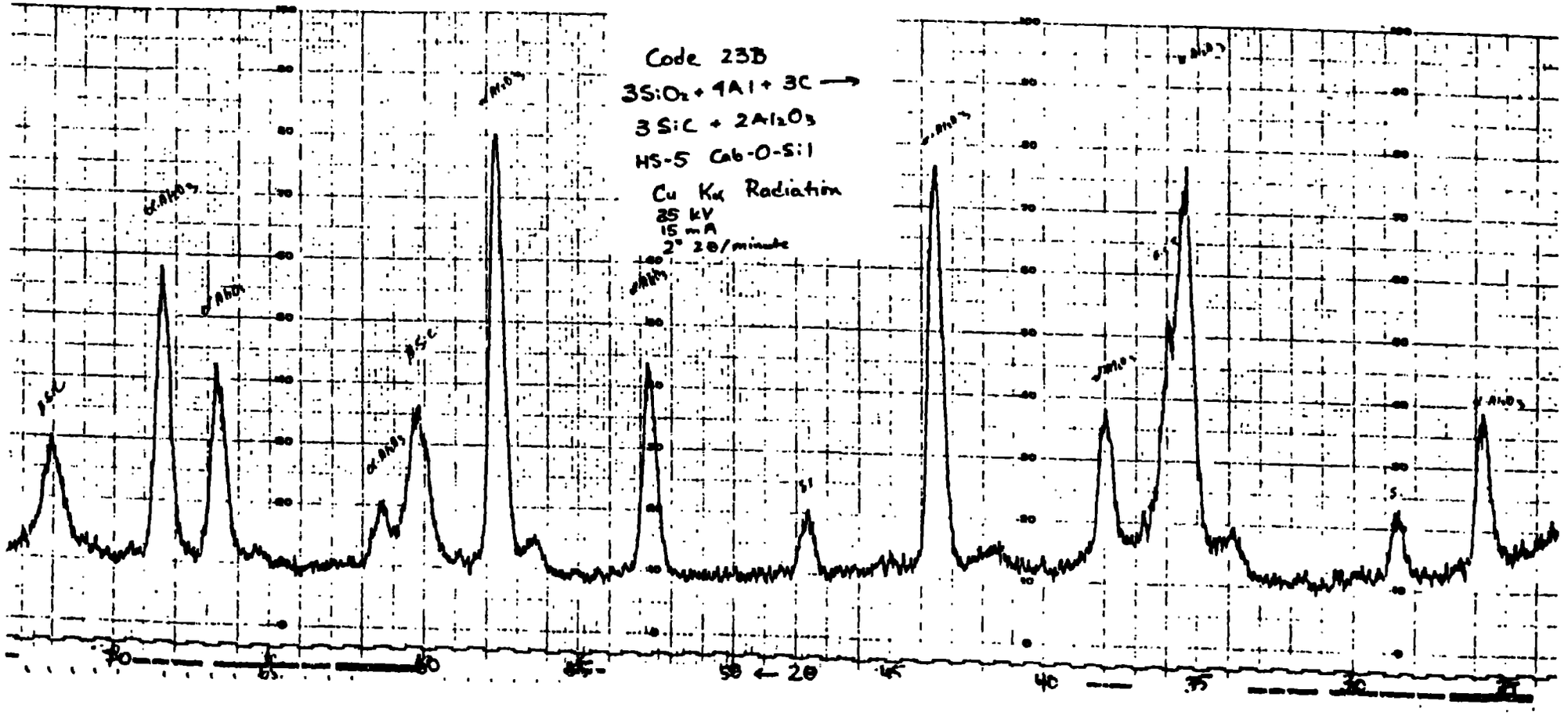

Fig. 11. XRD pattern for SiC-Al_2O_3 powder prepared by Reaction (4). A high purity fumed silica (Code 23B in Table 4) was used to make the SiC. Compare with Figure 10.

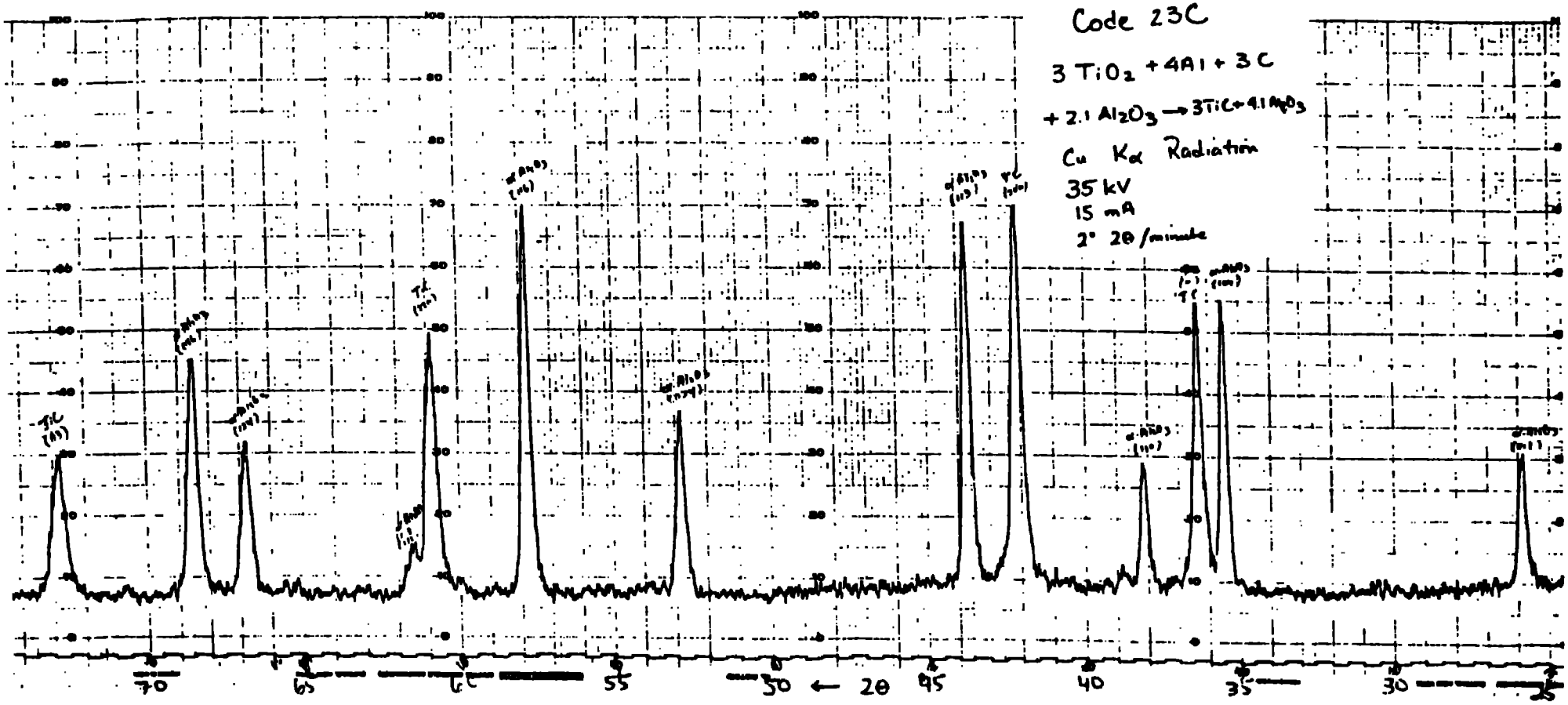

Fig. 12. XRD pattern of TiC-Al_2O_3 powder (Code 23C) synthesized using Reaction (5). Note that no intermetallics or free Ti are seen in the XRD pattern.

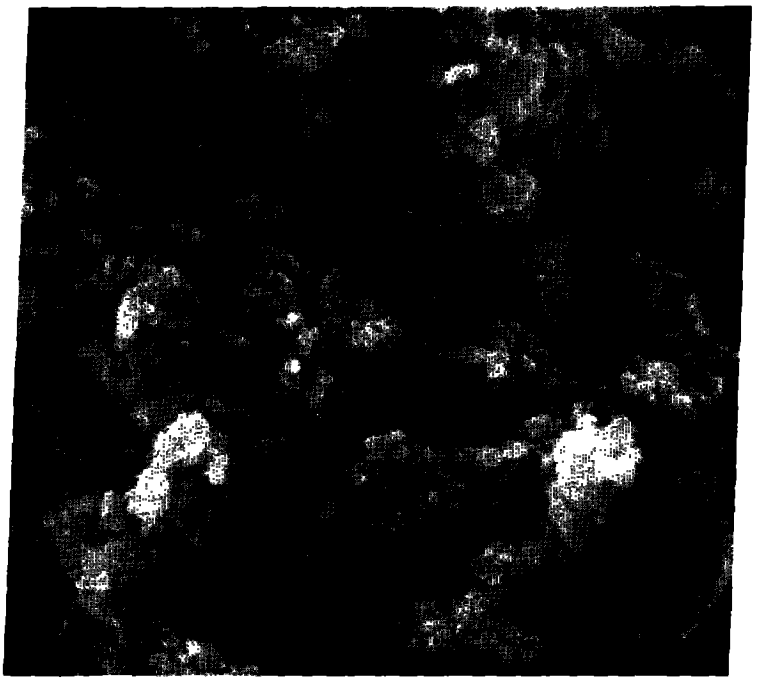

(a)

(b)

Fig. 13. SEM photomicrographs showing submicron particle size of TiC-Al_2O_3 powders synthesized by Reaction (5). Particle sizes range from 0.05 to 0.5 μm, with 0.3 μm being the mean particle size. (a) 4000X, (b) 30,000X.

TABLE 4. COMPOSITION OF ALUMINUM REDUCTANT POWDERS

Code	Composition (wt.%)					Phases Identified by XRD
	SiO_2	TiO_2[a]	Al[b]	Al_2O_3[c]	C[d]	
23A	55.3[e]	-	33.3	-	11.1	α-Al_2O_3, β-SiC, Si
23B	55.6[f]	-	33.3	-	11.1	α-Al_2O_3, β-SiC, Si
23C	-	40.0	18.0	36.0	6.0	α-Al_2O_3, TiC
23D	-	53.3	24.0	14.7	8.0	α-Al_2O_3, TiC
23E	-	62.4	28.2	-	9.4	α-Al_2O_3, TiC

[a] P-25 (50 m^2/g), Degussa AG (Frankfurt, Germany).

[b] Alcoa 123 (0.2-0.3 m^2/g), ALCOA (Pittsburg, PA).

[c] A-16 SG (5 m^2/g), ALCOA.

[d] Gulf Acetylene Black (65 m^2/g).

[e] Microsilica (94-98% SiO_2, 11 m^2/g), Elkem a/s (Voagsbygd, Norway).

[f] Cab-O-Sil HS-5 (324 m^2/g).

A paper (see enclosed copy) was prepared during the quarter and submitted for publication as a part of the Proceedings of the 9th Annual Conference on Composites and Advanced Ceramic Materials in Ceramic Engineering and Science Proceedings. The paper includes a table which shows the economics of Reaction (5) as compared to competing technologies. Reaction (4) will be similarly attractive.

In order to estimate the attractiveness of Reaction (1), a similar Table was prepared (see Table 5). Due to the higher cost of Mg, as compared to Al, and the additional acid leaching steps, the submicron SiC raw material costs are much more expensive than SiC-Al_2O_3 (or TiC-Al_2O_3) powders. The raw material costs of $10/kg are still attractive in today's market place if the powder can be sintered. High purity submicron SiC powder sells for $40/kg and 1-5 micron TiC sells for $20/kg. The major emphasis of the present effort at Ceramatec is determining whether sinterable SiC powder can be made using this approach.

SUMMARY

It has been conclusively demonstrated that submicron SiC, SiC-Al_2O_3, or TiC-Al_2O_3 can be made by starting with submicron oxides and carbon. It is not yet clear whether submicron materials can be made by reacting submicron carbon with elements (i.e., Reaction (3)) but it appears that the starting carbon size influences the final size of the product. The starting oxide particle size affects the amount of carbide formed, but more work is needed to clarify reaction kinetics. Efforts aimed at determining the reaction kinetics of gases evolved during the exothermic reactions have been postponed until a

TABLE 5. ECONOMICS OF SiC OR TiC PRODUCTION BY EXOTHERMIC REACTIONS

MATERIAL	PRICE PER Kg*
Carbon Black (C)	2.75
Hydrochloric Acid (HCl)	0.15
Hydrofloric Acid (HF)	5.90
Magnesium (Mg)	0.11
Silica (SiO_2)	1.65
Titania (TiO_2)	1.65

REACTION	COST ($) OF RAW MATERIALS TO SYNTHESIZE 1000 kg CARBIDE
$SiO_2 + 2\ Mg + C \rightarrow SiC + 2MgO$	8,070
Wash to remove MgO	1,080
Wash to remove SiO_2	950
Cost to produce SiC	10,100
$TiO_2 + 2Mg + C \rightarrow TiC + 2MgO$	702
Cost to produce SiC	

*Price from "Chemical Marketing Reporter", May 10, 1985 and Gulf Oil Chemicals Company

clearer understanding of the effect of initial particle size on reaction products is obtained. An investigation of the effect of atmosphere on reaction products was initiated. Economics for the recovery of submicron SiC from SiC-MgO powders are attractive if sinterable SiC can be made by adding dopants (i.e., B and Al) to the reacted powders.

SECTION V

Robert Behrens - Los Alamos National Lab. Los Alamos, New Mexico
John Margrave - Rice University, Houston, Texas

LASER-INDUCED SOLID-SOLID COMBUSTION PROCESSES

INTRODUCTION

The work described in this report covers the time period 1 February 1985-30 April 1985 and includes work performed as Los Alamos National Laboratory, Rice University, and the Houston Area Research Center (HARC).

SAMPLE PREPARATION

Table 1 summarizes pellets prepared at Los Alamos for laser ignition and mass spectrometer degassing experiments. Sources of the materials are as indicated at the end of the table.

Rice University also obtained the following samples from the Army Materials and Mechanics Research Center (AMMRC) for characterization by Fourier Transform Infrared Spectroscopy (FTIR):

- boron, 99% amorphous, less than 1 micron particle size (Gallard-Schlesinger, Lot No. 82821)
- boron, unspecified purity, crystalline, -325 mesh (Alfa Products, Lot No. 111583)
- titanium unspecified purity, -325 mesh (Alfa Products, Lot No. 042484).

MASS SPECTROMETRY

During degassing experiments, a major portion of condensible gas species (such as atomic metals) may be deposited on the walls of the vacuum system adjacent to the sample being heated. To facilitate cleaning, removable strain-less steel heat shields have been incorporated in the mass spectrometer vacuum system. These shields will capture (by condensation) a major portion of the condensible vapor species. The shields can be easily removed from the vacuum system and cleaned.

A factor of 10 increase in the mass spectrometer sensitivity and an increase in the stability of the mass scale were also achieved during this report by partially rewiring power supplies and improving grounding in order to minimize 60 cycle interference.

A new magnetic drive was installed on the sample holder position number 6 in order to improve the accuracy of sample positioning.

Work also continues to improve all aspects of the mass spectrometer/PDP-11 data acquisition software.

TABLE 1. LOS ALAMOS COMBUSTION SYNTHESIS SAMPLES

PELLET	GRAMS	PELLET WEIGHT INCHES	PELLET LENGTH INCHES	PELLET DIAMETER COMMENTS	COMPOSITION	PELLET
2-6-85	- 1	0.0671	0.0682	0.1888		Ti + $B_{1.5}$
	- 2	0.0308	0.0292	0.1888	slightly chipped	Ti + $B_{1.5}$
	- 3	0.0316	0.0324	0.1888		Ti + $B_{1.5}$
	- 4	0.0245	0.0263	0.1888		Ti + $B_{1.5}$
	- 5	0.0228	0.0236	0.1888		Ti + $B_{1.5}$
	- 6	0.0207	0.0243	0.1888		Ti + $B_{1.5}$
	- 7	0.0236	0.0245	0.1888	slightly chipped	Ti + $B_{1.5}$
	- 8	0.0249	0.0231	0.1888		Ti + $B_{1.5}$
	- 9	0.0287	0.0253	0.1888		Ti + $B_{1.5}$
	-10	0.0193	0.0203	0.1888		Ti + $B_{1.5}$
	-11	0.0776	0.0614	0.1888		Ti + C
	-12	0.0796	0.0603	0.1888		Ti + C
	-13	0.0765	0.0600	0.1888		Ti + C
	-14	0.0720	0.0573	0.1888		Ti + C
	-15	0.0429	0.0381	0.1888	slightly chipped	Ti + C
	-16	0.0475	0.0385	0.1888		Ti + C
	-17	0.0519	0.0417	0.1888		Ti + C
	-18	0.0472	0.0371	0.1888		Ti + C
	-19	0.0476	0.0373	0.1888		Ti + C
	-20	0.0474	0.0384	0.1888		Ti + C
	-21	0.0954	0.0685	0.1888		Zr + B
	-22	0.0768	0.0490	0.1888		Zr + B
	-23	0.0698	0.0491	0.1888		Zr + B
	-24	0.0768	0.0473	0.1888		Zr + B
	-25	0.0789	0.0477	0.1888		Zr + B
	-26	0.0597	0.0330	0.1888		Zr + B
	-27	0.0770	0.0471	0.1888		Zr + B
	-28	0.0575	0.0332	0.1888		Zr + B
	-29	0.0702	0.0390	0.1888		Zr + B
	-30	0.0620	0.0339	0.1888		Zr + B
2-11-85	- 1	0.0876	0.0396	0.1888		Zr + C
	- 2	0.0802	0.0378	0.1888		Zr + C
	- 3	0.0865	0.0412	0.1888		Zr + C
	- 4	0.0873	0.0422	0.1888		Zr + C
	- 5	0.0739	0.0361	0.1888		Zr + C
	- 6	0.0761	0.0369	0.1888		Zr + C
	- 7	0.0721	0.0343	0.1888		Zr + C
	- 8	0.0800	0.0383	0.1888		Zr + C
	- 9	0.0744	0.0358	0.1888		Zr + C
	-10	0.0740	0.0350	0.1888		Zr + C
	-11	0.0755	0.0229	0.1876		Hf + C
	-12	0.0699	0.0225	0.1876		Hf + C
	-13	0.0852	0.0266	0.1876		Hf + C
	-14	0.0729	0.0209	0.1876		Hf + C
	-15	0.0744	0.0225	0.1876		Hf + C
	-16	0.0814	0.0250	0.1876		Hf + C
	-17	0.0796	0.0250	0.1876		Hf + C

TABLE 1. LOS ALAMOS COMBUSTION SYNTHESIS SAMPLES (CONTINUED)

PELLET	GRAMS	PELLET WEIGHT INCHES	PELLET LENGTH INCHES	PELLET DIAMETER COMMENTS	COMPOSITION	PELLET
2-11-85	-18	0.0751	0.0223	0.1876		Hf + C
	-19	0.0837	0.0255	0.1876		Hf + C
	-20	0.0754	0.0239	0.1876		Hf + C
	-21	0.0587	0.0221	0.1876		Hf + B
	-22	0.0710	0.0253	0.1876		Hf + B
	-23	0.0671	0.0251	0.1876		Hf + B
	-24	0.0736	0.0247	0.1876		Hf + B
	-25	0.0687	0.0247	0.1876		Hf + B
	-26	0.0694	0.027	0.1876		Hf + B
	-27	0.0686	0.0260	0.1876		Hf + B
	-28	0.0792	0.0281	0.1876		Hf + B
	-29	0.0728	0.0245	0.1876		Hf + B
	-30	0.0696	0.0249	0.1876		Hf + B
	-31	0.0918	0.0619	0.1876		Ti + Lb
	-32	0.0809	0.0548	0.1876		Ti + Lb
	-33	0.0814	0.0562	0.1876		Ti + Lb
	-34	0.0788	0.0562	0.1876		Ti + Lb
	-35	0.0808	0.0662	0.1876		Ti + Lb
	-36	0.1196	0.0504	0.1876		Zr + Lb
	-37	0.1199	0.0508	0.1876		Zr + Lb
	-38	0.1195	0.0507	0.1876		Zr + Lb
	-39	0.1196	0.0508	0.1876		Zr + Lb
	-40	0.1197	0.0508	0.1876		Zr + Lb
2-19-85	- 1	0.0717	0.0504	0.1876		Ti
	- 2	0.0744	0.0508	0.1876		Ti
	- 3	0.0790	0.0509	0.1876		Ti
	- 4	0.0563	0.0785	0.1875		C + Lb
	- 5	0.0411	0.0507	0.1875		C + Lb
	- 6	0.0363	0.0421	0.1875		C + Lb
	- 7	0.1172	0.0503	0.1876		Zr
	- 8	0.1189	0.0504	0.1876		Zr
	- 9	0.1175	0.0504	0.1876		Zr
	-10	0.2194	0.0504	0.1876		Hf
	-11	0.2116	0.0503	0.1876		Hf
	-12	0.2156	0.0504	0.1876		Hf
	-13	0.0351	0.0506	0.1877		B
	-14	0.0317	0.0503	0.1877		B
	-15	0.0329	0.0507	0.1877		B
2-15-85	- 1	0.2102	0.1717	0.1877		Ti + C
	- 2	0.2361	0.1823	0.1877		Ti + C
	- 3	0.2494	0.1895	0.1877		Ti + C
	- 4	0.2403	0.1852	0.1877		Ti + C
	- 5	0.2447	0.1872	0.1877		Ti + C
	- 6	0.3791	0.1777	0.1875		Zr + C
	- 7	0.3824	0.1852	0.1875		Zr + C
	- 8	0.4104	0.1888	0.1875		Zr + C

TABLE 1. LOS ALAMOS COMBUSTION SYNTHESIS SAMPLES (CONTINUED)

PELLET	GRAMS	PELLET WEIGHT INCHES	PELLET LENGTH INCHES	PELLET DIAMETER COMMENTS	COMPOSITION	PELLET
2-15-85	- 9	0.4073	0.1875	0.1875		Zr + C
	-10	0.4098	0.1879	0.1875		Zr + C
	-11	0.1731	0.1629	0.1877		Ti + B
	-12	0.1871	0.1718	0.1877		Ti + B
	-13	0.1905	0.1771	0.1877		Ti + B
	-14	0.1956	0.1778	0.1877		Ti + B
	-15	0.2127	0.1884	0.1887		Ti + B
	-16	0.2090	0.1708	0.1875		Zr + Lb
	-17	0.3450	0.1709	0.1875		Zr + Lb
	-18	0.4424	0.2001	0.1875		Zr + Lb
	-19	0.4041	0.1898	0.1875		Zr + Lb
	-20	0.3939	0.1867	0.1875		Zr + Lb
	-21	0.2191	0.1793	0.1875		Ti + Lb
	-22	0.2155	0.1782	0.1875		Ti + Lb
	-23	0.2149	0.1690	0.1875		Ti + Lb
	-24	0.2333	0.1752	0.1875		Ti + Lb
	-25	0.2394	0.1761	0.1875		Ti + Lb
2-20-85	- 1	0.0830	0.0507	0.1878		Zr + Al_2O_3
	- 2	0.0919	0.0517	0.1878		Zr + Al_2O_3
	- 3	0.0838	0.0507	0.1878		Zr + Al_2O_3
	- 4	0.0919	0.0515	0.1878		Zr + Al_2O_3
	- 5	0.0924	0.0512	0.1878		Zr + Al_2O_3
	- 6	0.0571	0.050±	0.1877		Ti + Al_2O_3
	- 7	0.0916	0.0821	0.1877		Ti + AL_2O_3
	- 8	0.0730	0.0505	0.1877		Ti + Al_2O_3
	- 9	0.0625	0.0502	0.1877		Ti + Al_2O_3
	-10	0.0683	0.0506	0.1877		Ti + Al_2O_3
	-11	0.1166	0.0670	0.1877		Hf + Al_2O_3
	-12	0.1147	0.0681	0.1877		Hf + Al_2O_3
	-13	0.1142	0.0684	0.1877		Hf + Al_2O_3
	-14	0.1141	0.0672	0.1877		Hf + Al_2O_3
	-15	0.1210	0.0691	0.1877		Hf + Al_2O_3

Hf - Alfa Prod -325 MESH LOT# 00138
B - A. D. MacKay -325 MESH LOT# 1 Crystalline
C - Nat. Carbon Co. -325 MESH LOT# 12T
Ti - Alfa Prod. -325 MESH LOT# 042484
Zr - Alfa Prod -325 MESH LOT # 021182
Lb(Lampblack) - 200 MESH outgassed in vacuum

LASER IGNITION

A new set of sample holders has been made, which will allow secure mounting of the sample pellets while retaining the ability to photograph the sample from both ends and a side simultaneously. A design for a "split image" optical table has also been worked out. This table will allow us to obtain high speed movies of at least two, and possibly three, sides of the sample in the laser ignition experiments.

PYROMETRY

Work is progressing on development of a fast multi-color pyrometer. We have also built a prototype fast silicon-photodiode single color pyrometer with direct visual sighting. We have also obtained a 256 element linear CCD detector array which is intended for use in thermal profiling experiments.

KBr PELLET FTIR EXPERIMENTS

FTIR Experiments using KBr pellets containing the crystalline and amorphous boron and the titanium obtained from AMMRC were performed. To date, the sensitivity of the instrument has not been sufficient to allow conclusions to be made about impurity levels or chemical form of the impurities.

VISITS AND MEETINGS

George Hansen (graduate student, Rice University) visited Los Alamos on April 8 to discuss the work being performed at Rice and HARC. George presented a formal seminar to Los Alamos personnel on the mass spectrometer degassing studies.

We have arranged for George Hansen to spend the summer at Los Alamos to work on the DARPA SHS program. George's work this summer will focus on thermochemical modeling of the impurity chemistry of several chemical systems of interest. He will also be modeling the chemistry of thermite-type reactions of interest to determine if there are parameters (such as temperature, pressure) which can be adjusted to optimize formation of the desired product and minimize side reactions and incomplete reaction. Funding for this visit comes from the Los Alamos Materials Science and Technology Division.